This is to certify that the
thesis entitled

ISOTOPOLOGUE FRACTIONATION DURING MICROBIAL REDUCTION OF $N_2O$ IN SOIL

presented by

MALEE JINUNTUYA

has been accepted towards fulfillment
of the requirements for the

M.S. degree in Geological Sciences

Nathan E. Ostrom
Major Professor's Signature

May 9, 2007
Date

# ISOTOPOLOGUE FRACTIONATION DURING MICROBIAL REDUCTION OF $N_2O$ IN SOIL

By

Malee Jinuntuya

A THESIS

Submitted to
Michigan State Univeristy
in partial fulfillment of the requirements
for the degree of

MASTER OF SCIENCE

Department of Geological Sciences

2007

## ABSTRACT

ISOTOPOLOGUE FRACTIONATION DURING MICROBIAL REDUCTION OF $N_2O$ IN SOIL

By

Malee Jinuntuya

Reduction of $N_2O$ is a challenge to studies using isotope values to resolve global budgets and microbial sources of this critical greenhouse gas. Prior research has demonstrated that the difference in $\delta^{15}N$ between the central ($\alpha$) and outer ($\beta$) N atoms in the $N_2O$ can be used to distinguish $N_2O$ derived from nitrification and denitrification (Sutka et al., 2003; 2006; Toyoda et al., 2005). If intramolecular distribution of $^{15}N$, however, is altered during reduction, apportionment of $N_2O$ to nitrification and denitrification will be inaccurate. Isotopologue analyses of $N_2O$ within soil mesocosm experiments were used to investigate fractionation during $N_2O$ reduction at four levels of water filled pore space (WFPS) 60, 80, 100% (saturation) and 10% in excess. Soils were obtained from the Kellogg Biological Station Long Term Ecological Research Site (Michigan). Isotopic enrichment factors ($\varepsilon$) for $\delta^{15}N$, $\delta^{18}O$, $\delta^{15}N^{\alpha}$ and $\delta^{15}N^{\beta}$ ranged from -4.2 to -9.0, -12.5 to -23.6, -6.4 to -10.0 and -2.0 to -7.9, respectively. With the exception of site preference (SP), lower fractionation factors were observed at higher WFPS demonstrating the importance of diffusion in limiting the expression of enzymatic fractionation. Isotopic discrimination in SP was small and the $\varepsilon$ values varied between -4.5 and 0 ‰. Strong correlations were evident between $\delta^{18}O$ and $\delta^{15}N$ and $\delta^{18}O$ and $\delta^{15}N^{\alpha}$, with slopes of 2.7 and 2.0, respectively. These relationships (1) provide a definitive means for establishing that isotope effects during reduction are present and (2) may provide a means to determine the source signatures even when reduction occurs.

## DEDICATION

This work is dedicated to my parents, George K. Brown and Yaeko Jinuntuya, for believing that I am a scientist at heart.

## ACKNOWLEDGEMENTS

I would like to thank Dr. Nathaniel Ostrom for his support, guidance and patience throughout the course of this work. I would also like to thank the rest of my committee members, Drs. Grahame Larson and David Long for their invaluable advice and suggestions throughout my graduate career here at MSU. Many thanks go out to Drs. Robin Sutka, Hasand Gandhi and Peggy Ostrom, for their support and patience in teaching me. Robin, I can never thank you enough. Thanks for pushing me beyond the limit of what I thought I could do. You are truly instrumental to my success. Also, I would like to thank Dr. Lina Patino for all the encouragement she has provided, especially in times when I needed it most. Special thanks go out to my three partners in crime, Karen Tefend, Colleen McLean (TP) and Meredith Benedict. Your sheer enthusiasm and humor is what got me through this. I have earned more than colleagues; you are my friends for life. In addition to this fantastic group of people, I would like to acknowledge other graduate students in the department, for making life at MSU anything but boring. To my family, Karo, Yaeko, Sukanya, Angela and the Nortmans, you have been inspirational to me. This work is dedicated to you. Lastly, to my husband Dan, thanks for not letting me take the easy way out. This feat would not have been accomplished without your love and support.

## TABLE OF CONTENTS

## LIST OF TABLES

## LIST OF FIGURES

# INTRODUCTION

Increasing concerns over changes in global climate have warranted a closer examination of the microbial processes that produce the trace gas nitrous oxide ($N_2O$). Nitrous oxide, a greenhouse gas, is emitted into the troposphere from terrestrial ecosystems and plays an important role in altering stratospheric chemistry, including depletion of the ozone layer (Prather et al., 2003). In response to anthropogenic activities tropospheric $N_2O$ has been increasing at an average rate of 0.3 % per year since 1980 (IPCC, 2001; Prinn et al., 1990 and Rasmussen et al., 1986). Compared to the radiative forcing of carbon dioxide, $N_2O$ traps radiant energy 296 times more efficiently (IPCC, 2001), thereby contributing about 6 % to the overall global warming (Dalal et al., 2003). Even though $N_2O$ contributes only a fraction of the total warming effect, a small percentage increase in emission can potentially lead to a large accumulation of $N_2O$ in the troposphere as a result of its long residence time of approximately 120 years (Minschwaner et al., 1998; Olsen et al. 2001). Therefore, accurate apportionment of microbial sources is important in effectively mitigating $N_2O$ emissions.

Nitrous oxide is derived from both natural and anthropogenic sources. The major source of $N_2O$ flux from terrestrial ecosystems are microbial processes stimulated by agricultural activities, mainly application of nitrogen based fertilizers and tilling (Mosier and Kroeze, 1998; Nevison and Holland, 1997), which is found to stimulate microbial processes that produce this gas (Stein and Yung, 2003). Nitrification (aerobic) and denitrification (anaerobic) are the two primary microbial processes that produce and regulate $N_2O$ within the Earth's troposphere (Figure 1). Three separate pathways are

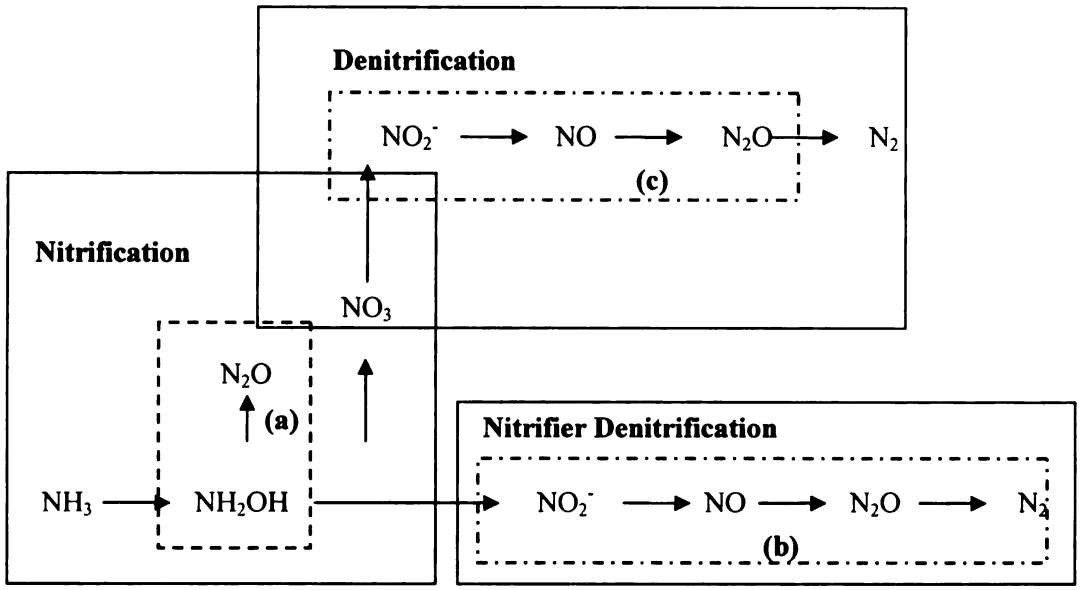


**Figure 1.** $N_2O$ production during nitrification and denitrification. The production of $N_2O$ can occur during oxidation of hydroxylamine (a), reduction of nitrite (b) and step-wise reduction of nitrate (c). Adapted from Wrage et al., 2001.

responsible for the microbial formation of $N_2O$: (1) oxidation of hydroxylamine during nitrification (Figure 1 a), (2) reduction of nitrite by nitrifier denitrification (Figure 1 b), and (3) through stepwise reduction of nitrate to $N_2$ during denitrification (Figure 1 c) (Wrage et al., 2001; 2004a). Therefore, nitrous oxide emissions from soils can be mitigated if the microbial process leading to its production is known.

Prior approaches to evaluate microbial production pathways have relied on the use of inhibitors or natural abundance isotope data. For example, acetylene is commonly used to block $N_2O$ reduction to $N_2$ to evaluate rates of denitrication (Groffman et al., 2006). The use of inhibitors, such as acetylene to evaluate $N_2O$ production, however, results in alteration of microbial activity and may not accurately reflect production pathways (Tilsner et al., 2003; Wrage et al., 2004b; 2004c). The natural abundance isotope approach is based on the difference in $\delta^{15}N$ between $N_2O$ and the substrates of nitrification and denitrification ($NH_4^+$ or $NO_3^-$, respectively). A difference of 60 ‰

indicates production from nitrification, whereas a difference of 30‰ reflects production from denitrification (Perez et al., 2000). Limitation of the substrates may reduce expression of fractionation. Thus, it is conceivable that nitrification can produce $N_2O$ that is depleted in $^{15}N$ by 30 ‰ relative to the substrate. Because of this non conservative behavior, bulk nitrogen isotope values ($\delta^{15}N$) may not definitively distinguish production pathway, and a conservative tracer is needed.

The distribution of $^{15}N$ within $N_2O$ molecule has been shown to be an effective tracer of the origins of $N_2O$ (Toyoda and Yoshida, 1999). Within the asymmetrical linear structure of the $N_2O$ molecule (N-N-O), the combination of five isotopes ($^{14}N$, $^{15}N$, $^{16}O$, $^{17}O$, $^{18}O$) yields 12 possible combinations of isotopes (isotopologues). The five most common isotopologues in order of abundance are: $^{14}N^{14}N^{16}O$, $^{15}N^{14}N^{16}O$, $^{14}N^{15}N^{16}O$, $^{14}N^{14}N^{17}O$, and $^{14}N^{14}N^{18}O$ (Yung and Miller, 1997). The abundance ratios of $^{15}N^{14}N^{16}O$ and $^{14}N^{15}N^{16}O$ isotopomers with respect to $^{14}N^{14}N^{16}O$ provide the basis to define the isotopic composition of central and outer N atoms as $\delta^{15}N^{\alpha}$ [1] and $\delta^{15}N^{\beta}$, respectively. The difference between $\delta^{15}N^{\alpha}$ and $\delta^{15}N^{\beta}$ yields position-specific isotopic information, and is commonly expressed as Site Preference (SP). Such information provides an additional insight into the pathways of microbial reactions (Sutka et al., 2003; 2006). Furthermore, the key advantages to the use of SP in contrast to bulk isotopes ($\delta^{15}N$ and $\delta^{18}O$) are (1) SP is independent of the isotopic composition of substrates, and therefore, is a

[1] Delta ($\delta$) expresses the isotopic composition of N and O in $N_2O$ with respect to Air (0 ‰) and Vienna Standard Mean Ocean Water (VSMOW) (0 ‰), and is defined by the equation,

$\delta = \left[\left(\frac{R_{sample}}{R_{s\,tan\,dard}}\right) - 1\right] \times 1000$, where R refers to the ratio of the heavy ($^{15}N$, $^{18}O$) to light ($^{14}N$, $^{16}O$) isotopes. Delta is expressed as per mil (‰).

conservative tracer, and (2) does not vary over the course of the reaction (Toyoda et al., 2005; Sutka et al., 2006).

Sutka et al. (2006), and Toyoda et al. (2005), demonstrated the effectiveness of $^{15}N$-SP as a tracer for the microbial sources during biogeochemical reactions in pure cultures. The SP in $N_2O$ produced during hydroxylamine oxidation (nitrification) (Figure 1 a) and nitrate reduction (denitrification) (Figure 1 c) have markedly distinct values of approximately 33 and 0‰, respectively. Reduction of nitrite by ammonia-oxidizing bacteria during nitrifier denitrification (Figure 1 b) yields a SP that was not distinguishable from $N_2O$ produced during nitrate reduction. Since $N_2O$ produced by both nitrifier denitrification and denitrification are reductive processes, they are combined and collectively termed "denitrification." The distinctive SP values associated with nitrification and denitrification allow microbial production of $N_2O$ to be differentiated.

While SP values characteristic of production by nitrification and denitrification have been identified, the affect of $N_2O$ reduction on SP remains uncertain. Recently changes in SP during $N_2O$ reduction have been established within pure microbial cultures (Ostrom et al., 2007). An isotopic enrichment factor of approximately 6‰ was observed. While small in magnitude, this value indicates that alteration of SP due to $N_2O$ reduction cannot be neglected in field studies using SP to evaluate microbial sources. Thus, in the presence of $N_2O$ reduction SP is not truly a conservative tracer.

Even though the isotopomer effect during $N_2O$ reduction has been identified in pure culture, the affect on SP by a natural soil microbial community has not been

established. The Rayleigh model has been the convention for defining isotope fractionation that occurs during many microbial reactions.

$$\delta_S = \delta_{SO} + \varepsilon \ln(C/C_O). \quad (1)$$

This equation quantifies the isotopic composition of the residual substrate ($\delta_s$) of a particular microbial reaction in relation to the initial substrate, the isotopic enrichment factor ($\varepsilon$), and the ratio of the natural log of observed concentration to the initial concentration ($C/C_0$). The $\varepsilon$, or the fractionation factor ($\alpha$) describes the fractionation during reactions that are restricted by masses of molecules and is defined as:

$$\alpha = \frac{k_2}{k_1}, \quad (2)$$

where $k_2$ and $k_1$ are the reaction rate involving the heavy and light isotopically substituted compounds and

$$\varepsilon = (\alpha - 1)\ 1000 \quad (3)$$

(Marriotti et al., 1981; 1988; Ostrom et al., 2002). The model assumes, in a biological process, fractionation is a single, unidirectional isotope reaction (Marriotti et al., 1981). However, in biological processes this assumption is not entirely accurate since, for instance reduction of $NO_3^-$ to $N_2$ occurs via a series of individual reaction steps (Figure 1) during denitrification (Firestone and Davidson, 1989). The magnitude of the expressed fractionation during reduction of $NO_3^-$ to $N_2$ is dependent upon which step in the reaction sequence is rate limiting. The most common factors limiting reduction are diffusion and the availability of enzymes to carry out each reduction step. The fractionation during diffusion is small; however, enzymatic fractionation tends to be large (Ostrom et al., 2002). For example, in water logged soil (100 % WFPS), $N_2O$ reduction is expected to

be limited by diffusion as the movement of the gas ($N_2O$) into the cell through water is a slow process, therefore net fractionation is expected to be small. On the other hand, at 60 % WFPS, diffusion is less likely to limit the supply of $N_2O$ to the cells but rather the enzymatic activity is the key rate limiting step. Under this condition the expressed fractionation is large. The magnitude of fractionation during $N_2O$ reduction will vary depending upon whether diffusion or enzymatic reduction is rate limiting. Thus, a low level of fractionation is observed when diffusion is limiting, and a high level when enzymatic reduction is significant (Ostrom et al., 2002). Consequently, the magnitude of isotopic fractionation is expected to decrease with increasing WFPS and the use of SP to evaluate sources of $N_2O$ production requires an understanding of the importance of this alteration.

Isotopic fractionation during microbial reduction of $N_2O$ was evaluated in this study at four levels of water soil-water content (60, 80, 100 and 110 % WFPS). By varying the WFPS, the relative importance of diffusion and enzymatic reduction were indirectly controlled. Soils used in this study w ere obtained from an uncultivated successional agricultural field plots within the W.K. Kellogg Biological Stations Long Term Ecological Research Site (KBS LTER) (Hickory Corners, MI). Uncultivated soil was used due to the rapid rate of $N_2O$ reduction previously observed (Ostrom et al., 2007). Since fractionation factors during $N_2O$ reduction are expected to differ with water content, fractionation at 60 % WFPS is expected to be the greatest. Knowledge of the magnitude of fractionation may provide a basis for correcting isotope shifts that occur during microbial denitrification and may allow for accurate apportionment of $N_2O$ fluxes from soils even when SP is altered by reduction.

## MATERIALS AND METHODS

Surface soil from an uncultivated successional field (treatment plot 7) was collected from the KBS LTER to construct experimental mesocosms. This plot is maintained as a native successional field following the abandonment of spring tillage in 1989. Soil was sieved through a screen with mesh size 2 mm, and air dried for 72 h and stored dry at 24 °C until the construction of mesocosms.

Soil mesocosms were constructed of 250 mL glass serum bottles and filled with approximately 40 g of dried soil. The amount of water added per gram of soil was determined based on the soil properties to obtain target WFPS values 60, 80, 100 (saturation), and 10 % in excess of saturation using the Gravimetric Water Content formula:

$$GWC = \frac{(WFPS \times TSP)}{\rho_b}, \tag{4}$$

where TSP is the total soil porosity (%) and $\rho_b$ is the bulk density of the soil (g/cm$^3$). The $\rho_b$ of air dried sieved soil was calculated using:

$$\rho_b = \frac{\text{weight of dry soil}}{\text{volume of core}}. \tag{5}$$

Total soil porosity is defined as:

$$TSP = \left[1 - \left(\frac{\rho_b}{\rho_s}\right)\right] \times 100, \tag{6}$$

where $\rho_s$ is the average particle density in most mineral soils and has the value of 2.65 g/cm$^3$ (Robertson et al., 1999). Once GWC was determined, filtered distilled water was

added according to method followed by Bergsma et al. (2002) into each mesocosm, to achieve to levels of 60, 80, 100 and 110 % WFPS. Each level of WFPS was prepared in triplicate.

Anaerobic conditions were created by purging each mesocosm with ultra high purity $N_2$ gas (99.999%). An initial incubation period that varied from 2-4 weeks was conducted to ensure the removal of any initial oxidized inorganic N by natural denitrification. During this time, 2.5 mL of headspace gas was sampled once or twice with a gas-tight syringe (Hamilton, Reno, NV) and the concentration of $N_2O$ was measured until production was no longer evident. Prior to removal of headspace gas, an equal amount of $N_2$ was injected into the mesocosms to ensure maintenance of atmospheric pressure. Sample gas was then stored in a 10 mL glass serum bottle purged with $N_2$, stoppered (using a rubber, butyl stopper), crimped, and analyzed on a multicollector Isoprime mass spectrometer interfaced to a Trace Gas system (GV Instruments, UK) (Sutka et al., 2003).

Once $N_2O$ production was no longer evident, a time series experiment was implemented over the course of 10-50 h. Initially, 250 μL of isotopically characterized $N_2O$ (substrate) was added with a gas-tight syringe to the mesocosm headspace. The reduction of $N_2O$ was monitored every 4 h until at least 60% of the $N_2O$ was reduced. At each time point, a gas sample of the headspace was taken and stored as described above. Samples were analyzed immediately (or within 8 h of sampling) on the mass spectrometer for concentration and isotopologue abundances ($\delta^{15}N$, $\delta^{18}O$, $\delta^{15}N^{\alpha}$ and $\delta^{15}N^{\beta}$). The Isoprime mass spectrometer has 5 collectors capable of monitoring simultaneously m/z 30, 31, 44, 45 and 46 that are required for measuring $N_2O$

isotopologues. The relative abundance of $^{15}N$ associated with N atom within the $N_2O$ molecule was obtained by analysis of the molecular ($N_2O$) and fragment ions ($NO^+$) produced within the ion source of the mass spectrometer (Toyoda and Yoshida, 1999). Isotope ratios were calculated from ion current ratios of $\delta^{45/44}$, $\delta^{46/44}$ and $\delta^{31/30}$ from which $\delta^{15}N$, $\delta^{18}O$, $\delta^{15}N^{\alpha}$ and $\delta^{15}N^{\beta}$ are calculated as described by Toyoda and Yoshida (1999). The $\delta^{15}N$, $\delta^{15}N^{\alpha}$ and $\delta^{18}O$ values of the $N_2O$ added to the mesocosm headspace were either 1.58, 14.90 and 41.70 ‰ (Tank A), respectively, or -0.93, 0.70 and 38.10 ‰ (Tank C), respectively. Two sets of experiment were conducted where the second experiment was employed two months subsequent to the first and the headspace was injected using isotopically characterized $N_2O$ standard from Tank C. Finally, SP for each treatment was determined as:

$$SP = {}^{15}N^{\alpha} - {}^{15}N^{\beta}. \quad (7)$$

# RESULTS

## Experiment 1

### Rates of $N_2O$ reduction

Headspace concentrations of $N_2O$ in all WFPS treatments (60, 80 and 100 %) manifested significant depletions as a function of time (Figure 2). The headspace concentrations in the three replicates for each treatment (60, 80 and 100 %) WFPS decreased from initial average concentrations for each treatment of 41.5, 40.4 and 42.7 μM/L to final concentrations of 18 (~60 % $N_2O$ depletion), 4 (~80 % depletion) and 15 μM/L (~70 % depletion), respectively (Figure 2 a,b,c and Table 1). Depletion of $N_2O$ within the 60 % WFPS treatment occurred in the span of 9 h for all replicates with the exception of replicate 1, where depletion of substrate $N_2O$ occurred almost instantaneously (Figure 2a). Over time, the rate of $N_2O$ reduction decreased with increasing WFPS in all treatments and depicted average rates of -73.3 ± 14.6, -44.9 ± 4.2 and -24.4 ± 3.5 mmol $N_2O$ $g^{-1}$ soil h for 60, 80 and 100 WFPS, respectively (Table 1).

### $N_2O$ isotopologue enrichment factors

Microbial reduction of $N_2O$ during the time series experiment within mesocosm treatments of 60, 80 and 100 % WFPS resulted in progressive enrichments of $^{15}N$ and $^{18}O$ in $N_2O$ (Table 2). The ε values for $^{15}N$, $^{18}O$, $^{15}N^{\alpha}$, $^{15}N^{\beta}$, and SP were determined based on the relationship between the isotopologue val ues and the natural log of the residual concentration data for 60, 80 and 100, experiment 1 substrate concentrations relative to the initial substrate concentrations (Eq. 1) (Figures 3, 4 and 5). The $\varepsilon^{15}N$ value for the

100 % WFPS mesocosm is -4.2±1.5 ‰. As WFPS decreases the ε values become more negative (-6.0±0.3 ‰ and -7.8±0.7 ‰ for 80 and 60 WFPS, respectively). The same trend of decreasing fractionation with increasing WFPS is also evident in $\varepsilon^{18}O$, $\varepsilon^{15}N^{\alpha}$ and $\varepsilon^{15}N^{\beta}$. Changes in εSP as a function of WFPS are not evident and are minimal, varying between -1 and -2 ‰ (Table 2).

**TABLE 1.** Headspace concentrations, microbial reduction rates of $N_2O$ and substrate depletion expressed as percent for 60, 80 and 100 %WFPS. The results represent data obtained from three replicates (R1, R2 and R3) during time series experiment.

| WFPS (%) | | Total Elapsed (h) | Rates (mmol $N_2O$ $g^{-1}$ soil $h^{-1}$) | [$N_2O$] Depleted (%) |
|---|---|---|---|---|
| 60R1 | | 7 | -84.3 | 53 |
| 60R2 | | 8 | -56.0 | 54 |
| 60R3 | | 9 | -76.2 | 63 |
| | AVG | | -73.3 | 57 |
| | STD | | 14.6 | 5 |
| 80R1 | | 17 | -40.1 | 67 |
| 80R2 | | 18 | -47.0 | 87 |
| 80R3 | | 17 | -47.6 | 80 |
| | AVG | | -44.9 | 78 |
| | STD | | 4.2 | 10 |
| 100R1 | | 28 | -28.4 | 71 |
| 100R2 | | 28 | -21.9 | 63 |
| 100R3 | | 28 | -22.8 | 63 |
| | AVG | | -24.4 | 66 |
| | STD | | 3.5 | 5 |

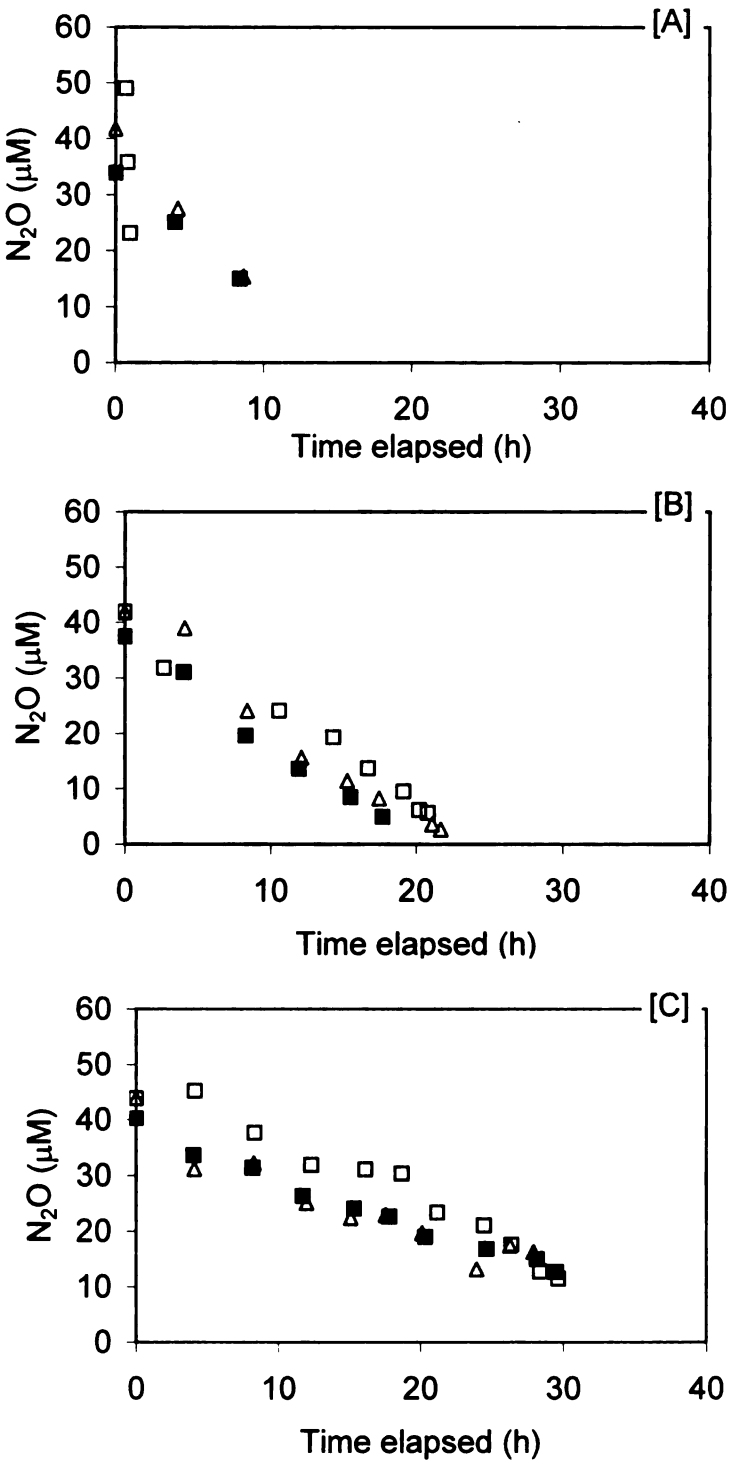


**FIGURE 2.** $N_2O$ headspace concentration as a function of time for 60 (a), 80 (b) and 100 % WFPS (c), experiment 1 for replicate mesocosms 1 (open square) , 2 (close square) and 3 (open triangle).

**TABLE 2.** The ε values for time series experiment 1 at 60, 80 and 100 % WFPS during microbial reduction of $N_2O$ as determined from the Rayleigh equation (Eq. 1). The value for εSP is determined as a difference between $\varepsilon^{15}N^{\alpha}$ and $\varepsilon^{15}N^{\beta}$ (Toyoda et al., 2005).

| WFPS (%) | ε $^{15}$N-bulk | ε $^{18}$O | ε $^{15}N^{\alpha}$ | ε $^{15}N^{\beta}$ | ε SP |
|---|---|---|---|---|---|
| 60R1 | -7.9 | -19.8 | -9.0 | -6.9 | -2.2 |
| 60R2 | -8.5 | -19.8 | -11.5 | -5.5 | -6.0 |
| 60R3 | -7.0 | -17.6 | -8.5 | -5.5 | -3.1 |
| AVG | -7.8 | -19.1 | -9.7 | -5.9 | -3.8 |
| STD | 0.7 | 1.3 | 1.6 | 0.8 | 2.0 |
| 80R1 | -6.2 | -15.8 | -7.3 | -5.2 | -2.1 |
| 80R2 | -6.0 | -15.7 | -7.5 | -4.5 | -3.0 |
| 80R3 | -5.6 | -14.0 | -7.5 | -3.8 | -3.7 |
| AVG | -6.0 | -15.2 | -7.4 | -4.5 | -2.9 |
| STD | 0.3 | 1.0 | 0.1 | 0.7 | 0.8 |
| 100R1 | -5.9 | -16.3 | -7.4 | -4.3 | -3.1 |
| 100R2 | -3.7 | -12.5 | -6.8 | -0.7 | -6.1 |
| 100R3 | -3.0 | -8.8 | -5.1 | -0.9 | -4.2 |
| AVG | -4.2 | -12.5 | -6.4 | -2.0 | -4.5 |
| STD | 1.5 | 3.8 | 1.2 | 2.1 | 1.5 |

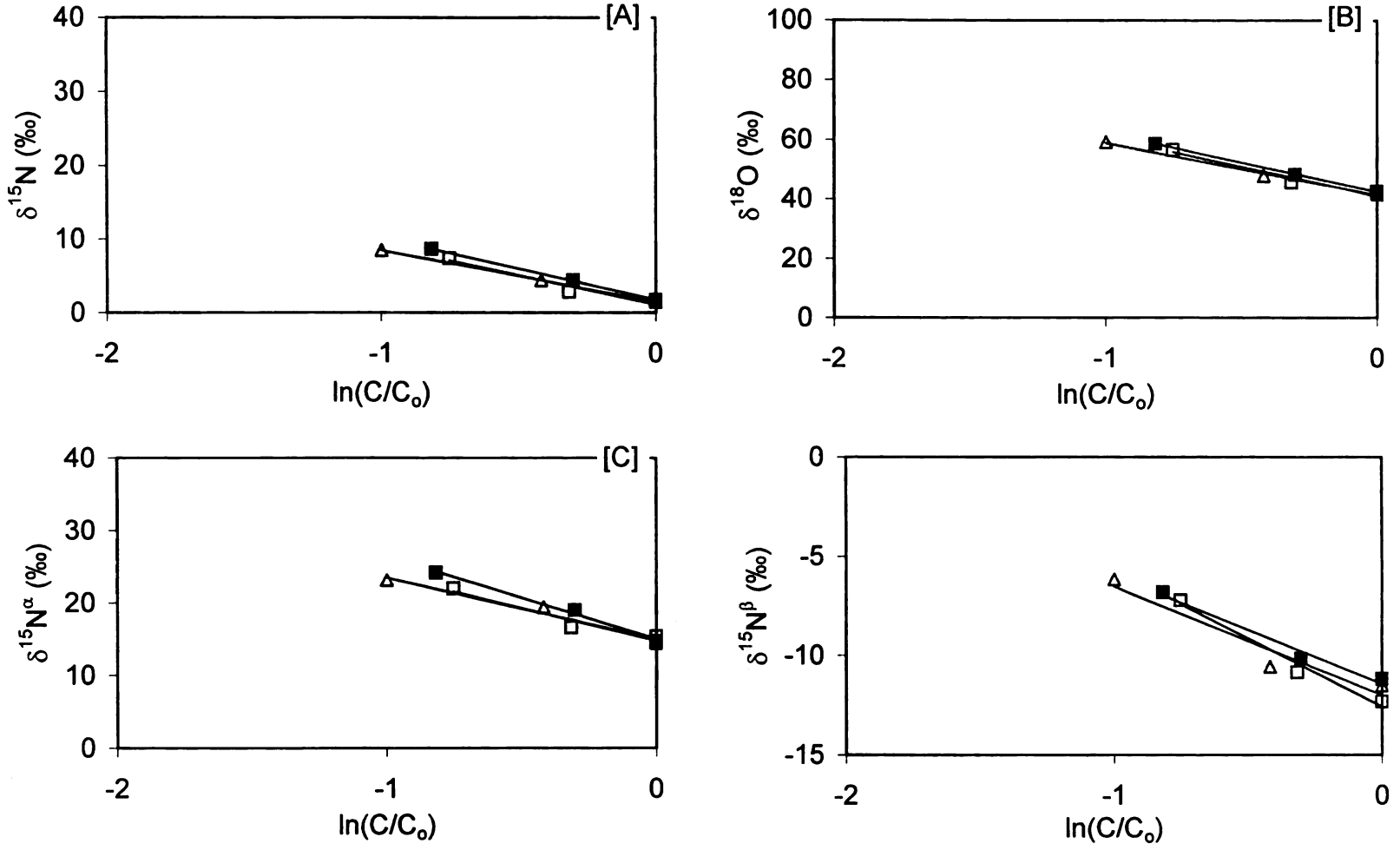


**FIGURE 3.** Isotopologue values as a function of $\ln(C/C_o)$ for 60 % WFPS, experiment 1 for replicate 1 (R1, open square), replicate 2 (R2, closed square) and replicate 3 (R3, open triangle). The slope of these relationships defines ε (Eq. 1). The $r^2$ values in all cases are ≥ 0.93.

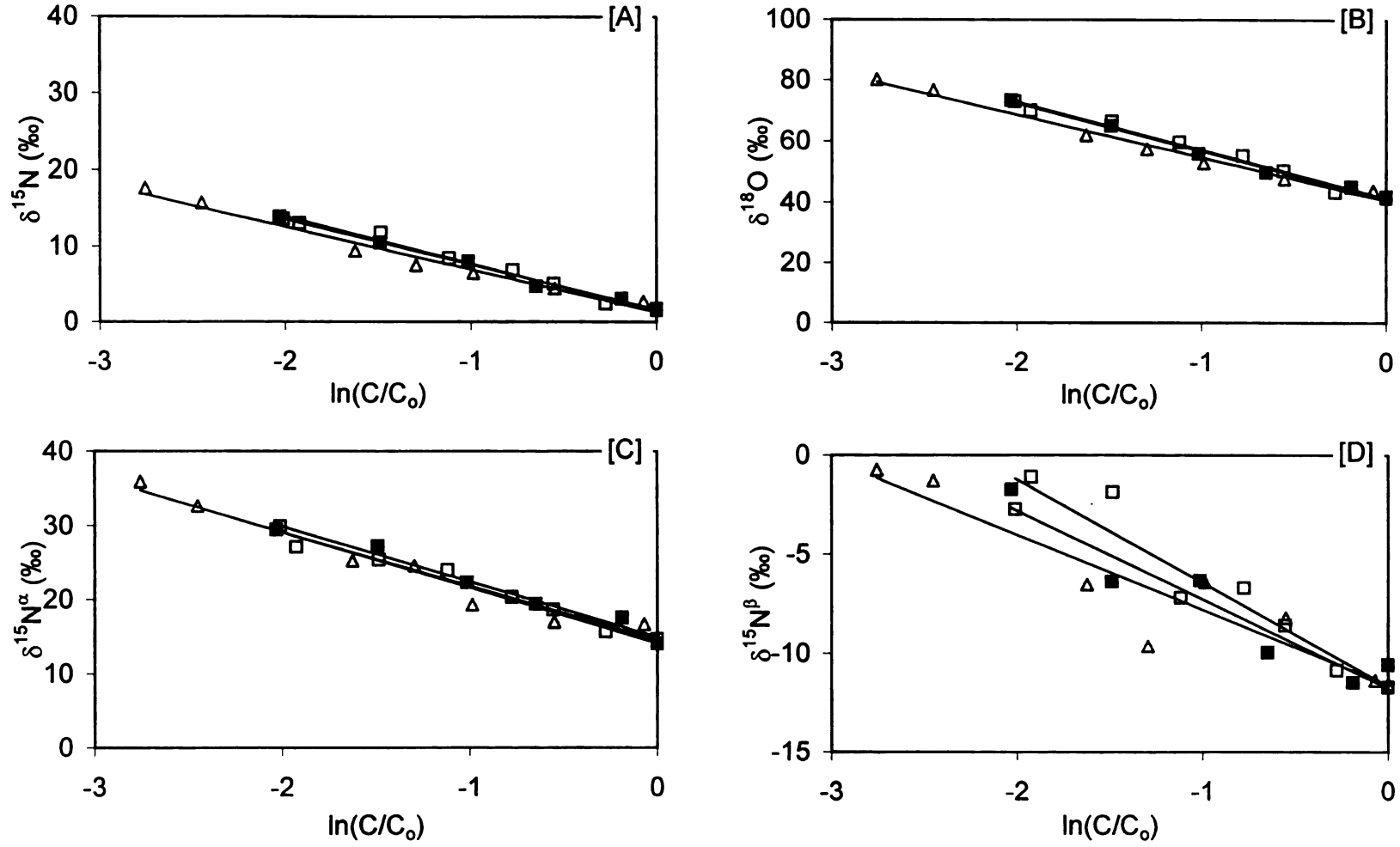


**FIGURE 4.** Isotopologue values as a function of $\ln(C/C_o)$ for 80 % WFPS. The slope of these relationships defines ε (Eq. 1). The $r^2$ values in all cases are ≥ 0.90.

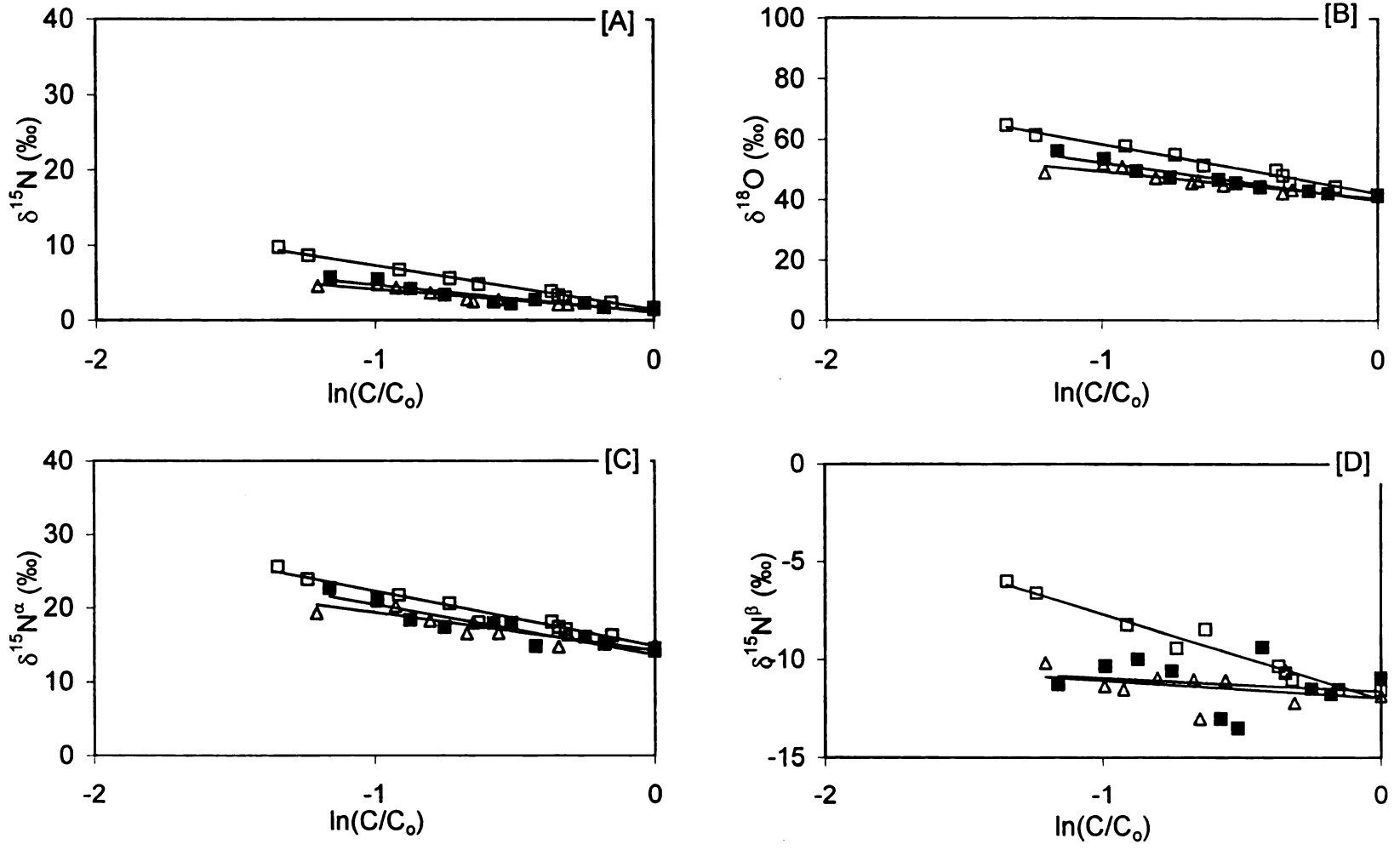


**FIGURE 5.** Isotopologue values as a function of $\ln(C/C_o)$ for 100 % WFPS. The slope of these relationship defines ε (Eq. 1) With the exception of $\delta^{15}N^{\beta}$, the $r^2$ values in all cases are ≥ 0.80. The $r^2$ values for $\delta^{15}N^{\beta}$ are 0.96 (R1), 0.04 (R2) and 0.15 (R

## Experiment 2

### Rates of $N_2O$ reduction

A second $N_2O$ reduction experiment was conducted two months subsequent to the first experiment but using the same soil sample and identical procedures as the first experiment. Two treatment conditions were conducted for the second experiment; 60 and 110 % WFPS. A saturation level of 60% was repeated in experiment 2 because the rapid rate of reduction in the first experiment resulted in a limited number of data points. A saturation condition of 110 % WFPS was conducted to study isotopologue fractionation during reduction under a supersaturated condition. The concentration of $N_2O$ in the 60 and 110 % WFPS mesocosms declined as a function of time, however, the rates of reduction (-16 and -21 mmol $N_2O$ $g^{-1}$ soil h for 60 and 110 %, respectively) was much lower than those observed in experiment 1 (Figure 6, Tables 3).

### $N_2O$ isotopologue enrichment factors

Strong correlations were evident between the natural log of the initial substrate concentration divided by to the residual concentration and all isotopologue values during the 60 and 110 % WFPS experiments (Figures 7). Such strong linear correlations

**TABLE 3.** Concentration and reduction rate of $N_2O$ in soil mesocosms for 60 and 110 WFPS, during time series experiment 2. $N_2O$ depletion, expressed as percent, reflects the amount of substrate reduced within the headspace samples in each soil mesocosm treatment.

| WFPS (%) | Total Elapsed hour | Rates (mmol $N_2O$ $g^{-1}$ soil $h^{-1}$) | $N_2O$ depleted (%) |
|---|---|---|---|
| 60 | 59 | -15.7 | 86 |
| 110 | 53 | -21.0 | 91 |

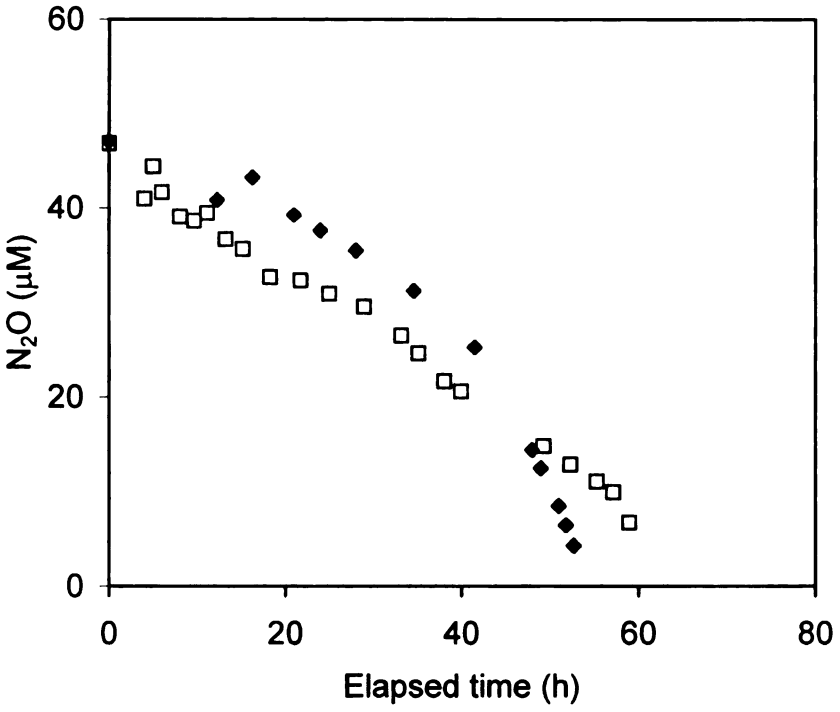


**Figure 6.** Concentration of $N_2O$ in soil mesocosms for 60 (open square) and 110 % (closed diamond) WFPS in experiment 2 as a function of time expressed in μM.

**TABLE 4.** The ε values for 60 and 110 % WFPS during $N_2O$ reduction, experiment 2. The ε values represent values obtained from the slope of the natural log plot with isotope values as a function of natural log of residual substrate concentration (C) relative to initial substrate concentration ($C_0$).

| WFPS (%) | ε $^{15}N$ | ε $^{18}O$ | ε $^{15}N^{\alpha}$ | ε $^{15}N^{\beta}$ | ε SP |
|---|---|---|---|---|---|
| 60 | -9.0 | -23.6 | -10.0 | -7.9 | -2.1 |
| 110 | -5.3 | -15.9 | -5.3 | -5.3 | 0.0 |

corroborate the use of the Rayleigh model to determine the isotopic enrichment factors (Eq. 1) (Table 4). The ε values for 60 WFPS were -9.0, -23.6, -10.0, -7.9, and -2.1 ‰ and -5.3, -15.9, -5.3, -5.3 and 0.0 ‰ for 110 WFPS (Table 4). Similar to the initial experiment conducted two months prior, the ε values for all isotopologues in the second experiment decrease with increasing WFPS with the exception of SP. The magnitude of the ε values during $N_2O$ reduction for the 60 and 110 % WFPS mesocosms in experiment 2 were slightly less than those observed in experiment 1 (Table 2). Additionally, in contrast to the first experiment, εSP for 60 % WFPS mesocosm exhibited a smaller shift (-3.8 vs -2.1 ‰) while the εSP value for the 110 % WFPS mesocosm was 0 ‰. The lack of variation in εSP under super saturated condition indicates that no observable fractionation had occurred and there was no change in the relative isotopic compositions of the α and β positions during reduction.

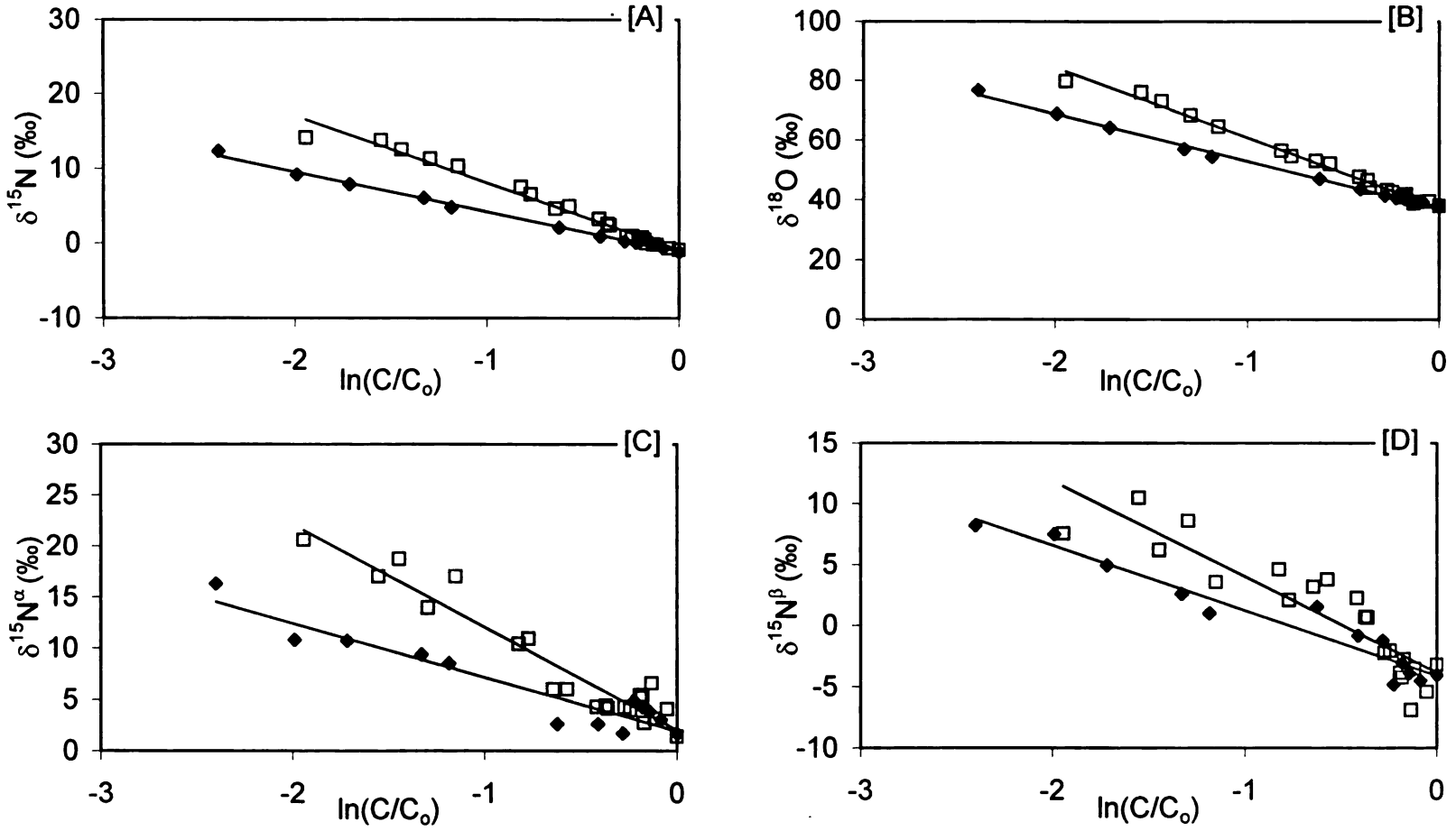


**Figure 7.** Isotopic compositions for $\delta^{15}N$, $\delta^{18}O$, $\delta^{15}N^{\alpha}$, $\delta^{15}N^{\beta}$ and SP for 60 (open square) and 110 % (closed diamond) WFPS, experiment 2. Plots A through D represents isotope values obtained from the natural log plot. The slope of the line in the natural log plot is the fractionation (enrichment) factor ($\varepsilon$) by the Rayleigh model. The SP values were calculated based on the difference between the $\delta^{15}N^{\alpha}$ and $\delta^{15}N^{\beta}$ and the resulting values are be shown in Table 4. The $r^2$ values in all cases are $\geq 0.82$.

**Relationships between $\delta^{18}O$ and $\delta^{15}N$ and $\delta^{18}O$ and $\delta^{15}N^{\alpha}$**

While ε values are clearly variable as function of WFPS and between experiments 1 and 2, there are consistent relationships between isotopologue values. For example, in all treatments there are strong correlations between $\delta^{18}O$ and $\delta^{15}N$ values with an average slope of 2.7 ± 0.2 (Table 5, Figure 8a, 9a). Similarly, consistent relationships are evident between $\delta^{18}O$ and $\delta^{15}N^{\alpha}$ with an average slope of 2.0 ± 0.3 (Table 5, Figure 8b, 9b).

**TABLE 5.** Slopes of the relationship between $\delta^{18}O$ vs. $\delta^{15}N$ and $\delta^{18}O$ vs. $\delta^{15}N^{\alpha}$ for 60, 80 and 100 % WFPS, experiment 1, and 60 and 110 % WFPS, experiment 2, during $N_2O$ reduction. All treatments in experiment 1 were conducted in triplicate. Experiment 2 was not replicated.

| | WFPS (%) | $\delta^{18}O$ vs $\delta^{15}N$ | $\delta^{18}O$ vs $\delta^{15}N^{\alpha}$ |
|---|---|---|---|
| Experiment 1 | 60R1 | 2.5 | 2.2 |
| | 60R2 | 2.3 | 1.7 |
| | 60R3 | 2.5 | 2.0 |
| | 80R1 | 2.5 | 2.2 |
| | 80R2 | 2.6 | 2.1 |
| | 80R3 | 2.4 | 1.8 |
| | 100R1 | 2.8 | 2.2 |
| | 100R2 | 3.2 | 1.71 |
| | 100R3 | 2.9 | 1.64 |
| Experiment 2 | 60 | 2.6 | 2.2 |
| | 110 | 2.9 | 2.7 |
| AVG | | 2.7 | 2.0 |
| STD | | 0.2 | 0.3 |

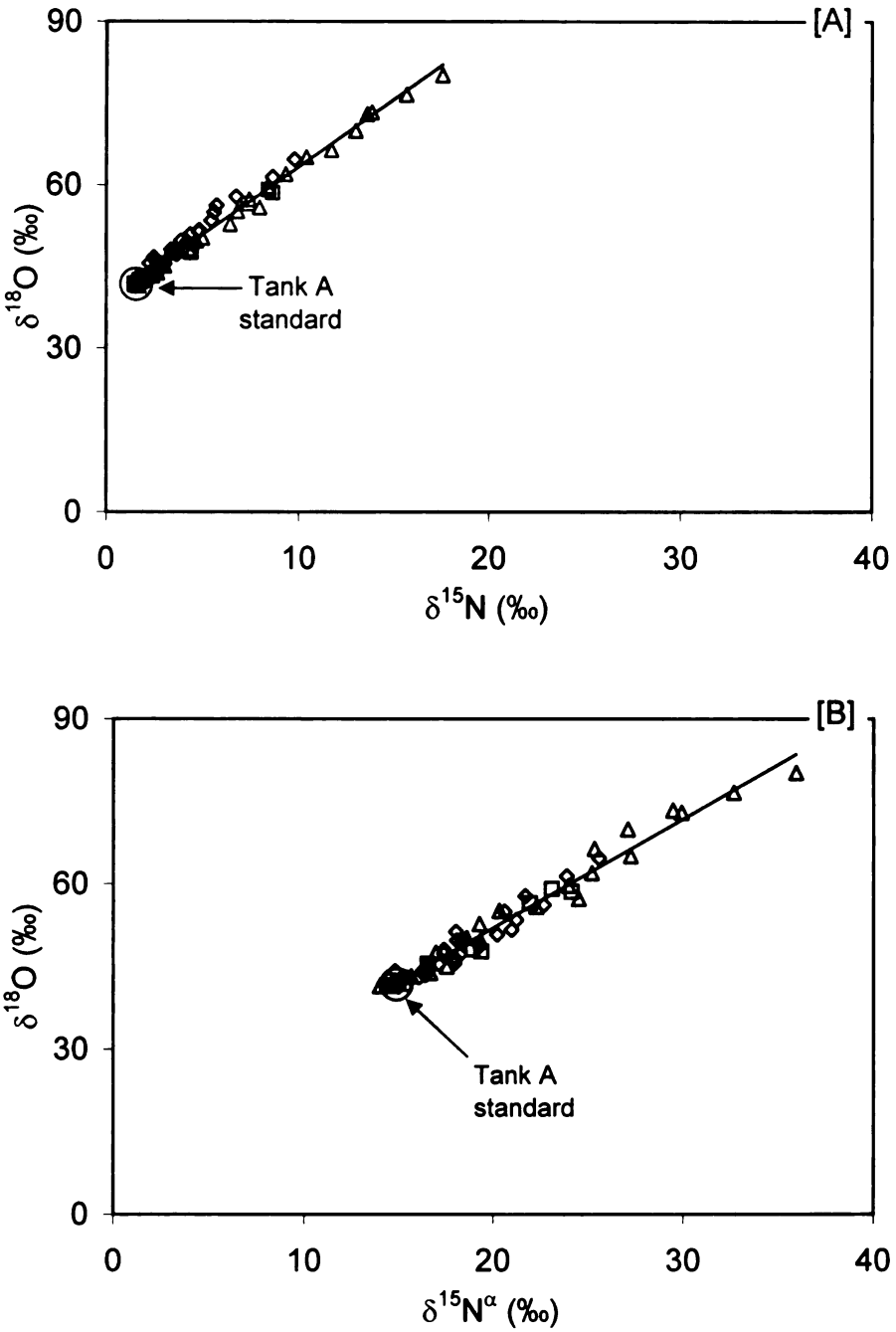


**Figure 8.** $\delta^{18}O$ as a function of $\delta^{15}N$ (A) and $\delta^{15}N^{\alpha}$ (B) for experiment 1 at 60 (open square), 80 (open triangle) and 100 % (open diamond) WFPS. The initial isotopologue values represent values from Tank A standard (open circle) of $N_2O$ that was added to the mesocosm headspace to initiate the experiment. Values for $r^2$ and p (t-test) in all cases are greater than 0.90 and less than 0.01, respectively.

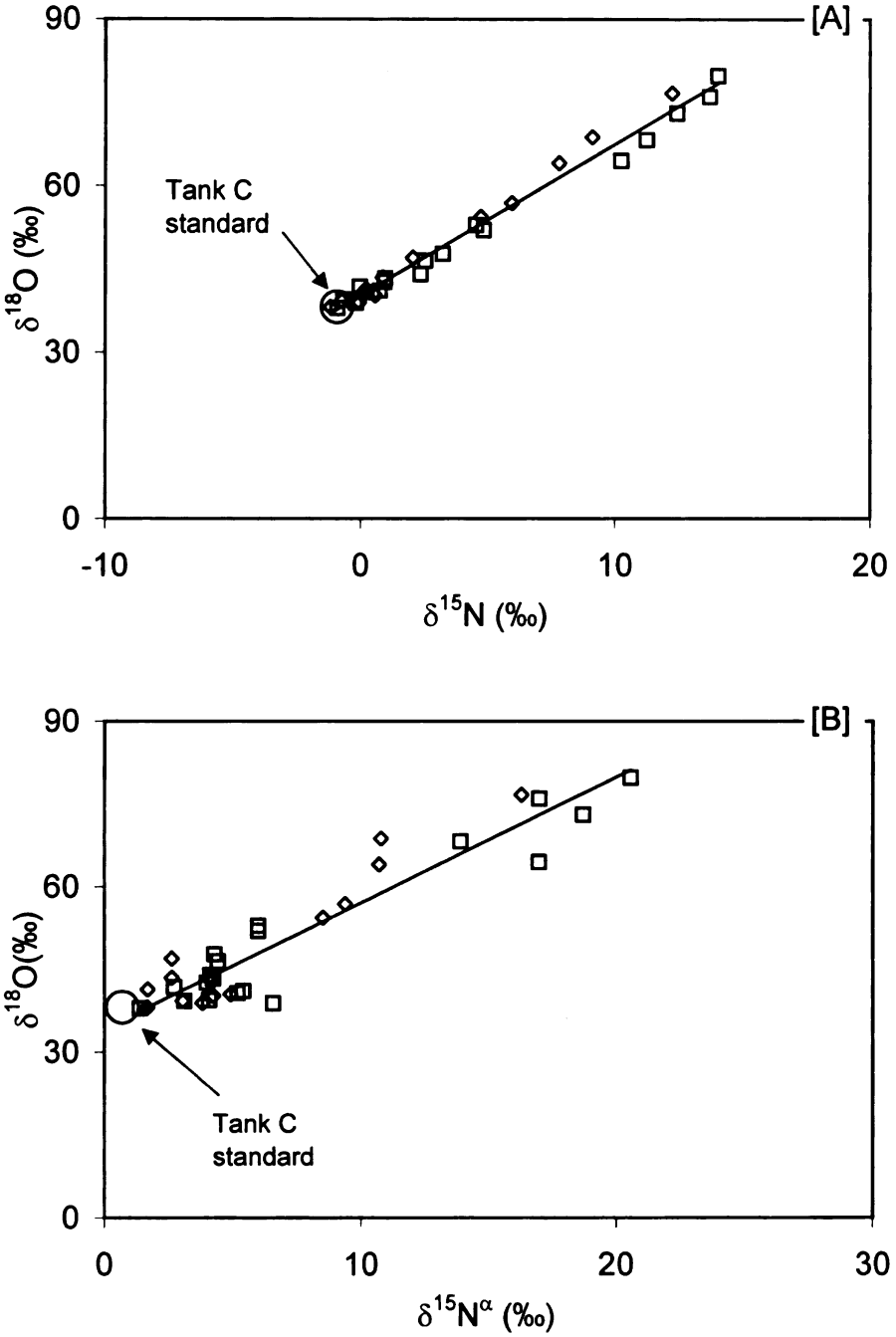


**Figure 9.** $\delta^{18}O$ as a function of $\delta^{15}N$ (A) and $\delta^{15}N^{\alpha}$ (B) for experiment 2 at 60 (open square) and 100 % (open diamond) WFPS. The initial isotopologue values represent values from Tank C standard (open circle) of $N_2O$ that was added to the mesocosm headspace to initiate the experiment. Values for $r^2$ and p(t-test) in all cases are equal to or greater than 0.90 and less than 0.01, respectively.

# DISCUSSION

## Isotopic effects on $N_2O$ during $N_2O$ reduction

Owing to complexity of natural microbial communities, published isotopologue enrichment factors for $N_2O$ reduction in soils has not been chronicled as extensively as in pure culture (Yoshida et al., 1984; Wahlen and Yoshinari, 1985; Yamazaki et al., 1987; Barford et al., 1999; Cavagelli and Robertson, 2001; Sutka et al., 2005, Ostrom et al., 2007). A challenge to isotope studies is that ε values for many microbial processes, notably $N_2O$ reduction tend to be variable (Mandernack et al., 2000; Ostrom et al., 2007). Microbial processes are commonly multi-step reactions, which violates the fundamental requirements of the Raleigh model (Eq. 1) that is designed for a single step uni-directional reaction. The net fractionation expressed during a microbial process tends to be the step that is rate limiting (Marrioti et al., 1988; 1981, Ostrom et al., 2007). For $N_2O$ reduction, the key rate limiting steps are diffusion (little fractionation) and enzymatic reduction (large fractionation). By varying the WFPS, this study was able to determine the importance of diffusion in controlling isotopic fractionation during $N_2O$ reduction.

In this study, $\varepsilon^{15}N$ and $\varepsilon^{18}O$ values for reduction of $N_2O$ in soil mesocosms at all levels of WFPS were -9.0 to -4.2 ‰ and -23.6 to -12.5 ‰, respectively. These isotope effects are generally small relative to other processes in the nitrogen cycle. For examples, $N_2O$ production by nitrification and denitrification has reported ε values of -68 and -28.6 ‰, respectively (Yoshida, 1988; Barford et al., 1999). Such differences reflect the unique behavior of isotopes during contrasting enzymatic reactions (Schmidt et al., 2004). Similarly, enzymatic reduction of $N_2O$ in pure cultures has been known to

produce ε values as high as -39 ‰ (Yamazaki et al., 1987) for $^{15}N$ and -42 ‰ (Wahlen and Yoshinari, 1985) for $^{18}O$. Yamagishi et al. (in press) also noted that fractionation during reduction of $N_2O$ in the eastern tropical North Pacific and the Gulf of California was expressed to a large degree and demonstrated slightly higher ε values than those collected from soils (-11.6 ± 1.0 for $\delta^{15}N$ and -30.5 ± 3.2 ‰ for $\delta^{18}O$). At the low end of the of the spectrum, incubation of landfill cover soils produced $\varepsilon^{15}N$ and $\varepsilon^{18}O$ of -2.4 and -4.9 ‰ (Mandernack et al., 2000), respectively. Isotopic discrimination for $\varepsilon^{15}N$ and $\varepsilon^{18}O$ in other soil studies is as large as -9.2 and -25.1 ‰ (in soil mesocosms at a single saturation level) (Ostrom et al., 2007), -9.8 and -24.9 ‰ (forest soils) (Menyailo and Hungate, 2006), respectively. These results suggest that isotopic discrimination in soils is expressed to a lesser degree than in pure cultures and oceans.

In microbial processes that consist of more than one reaction step, it is the rate limiting step that controls the observed fractionation for the entire process. Diffusion in general is associated with little to no fractionation (Brandes and Devol, 1997). Enzymatic fractionation tends to be quite large, and is likely the predominant factor controlling the large degree of discrimination observed for $N_2O$ reduction in pure culture (Wahlen and Yoshinari, 1985; Yamazaki et al., 1987). If the supply of substrate to the enzyme is limiting, then all of the substrate is converted to the product and no fractionation is observed. If the substrate is not limiting, however, the enzymatic fractionation tends to be fully expressed. Diffusion is the predominant factor in controlling the supply of substrate to the enzyme where $N_2O$ reduction occurs. The relative importance of the rate of diffusion and enzymatic reduction ultimately controls the observed or net isotopic fractionation. Thus, when diffusion across the cell boundary

is the rate limiting step, the observed fractionation for $N_2O$ reduction tends to be small. This is in contrast to when diffusion is not rate limiting, the overall fractionation tends to be large. In this study, the importance of diffusion was indirectly controlled by adjusting the WFPS. The trend of decreasing ε values with increasing WFPS is consistent with the importance of diffusion as outlined above (Tables 2 and 4). Diffusion is not the only factor controlling the net fractionation. The enzyme activity can vary depending on the supply of electron donor (organic carbon) or enzyme abundance. Thus, net fractionation varies depending upon the relative rates of diffusion versus enzyme activity.

With the exception of SP, all mesocosm treatments demonstrated consistent declines in the ε values for $\delta^{15}N$, $\delta^{18}O$, $\delta^{15}N^{\alpha}$, $\delta^{15}N^{\beta}$ (Tables 2 and 4) with increases in WFPS (60, 80, 100 and 110 %). This is consistent with reduction of enzyme activity due to diffusion limiting the transport of $N_2O$ into the cell. In contrast, there appeared to be no apparent relationship between SP and WFPS. The resulting ε values for SP for experiments 1 and 2 appear to be independent of the saturation conditions; -3.8 ‰ (60 %, experiment 1), -2.9 ‰ (80 %, experiment 1), -4.5 ‰ (100 %, experiment 1), -2.1 ‰ (60 %, experiment 2) and 0 ‰ (110 %, experiment 2). However, the ε values of SP during $N_2O$ reduction were small and only ranged between approximately 0 and -5 ‰. A trend may have been present but likely could not be resolved because the small ε values observed approach the experimental uncertainty (± 0.8 to ± 2.0, tables 2 and 4).

Comparison of experiments 1 and 2 yielded some disagreement in the ε values for each level of WFPS. The ε values in the second 60 % WFPS experiment were larger than in experiment 1; -9.0 vs -7.8 ‰ for $^{15}N$, -23.6 vs 19.1 ‰ for $^{18}O$ , -10.0 vs -9.7 ‰ for $^{15}N^{\alpha}$ and -7.9 vs -5.9 ‰ for $^{15}N^{\beta}$. Experiment 2 was repeated two months subsequent

to the initial experiment with the intention of obtaining supplementary isotope data. However, the rate of reduction was significantly slower in experiment 2, approximately -20 mmol $g^{-1}$ soil $h^{-1}$ as opposed to -73 mmol $g^{-1}$ soil $h^{-1}$. A slower rate of reduction possibly allowed greater expression of enzymatic fractionation as evidenced by the higher ε values in the 60% WFPS of experiment 2. A key plausible explanation for the disparity between the first and second 60 % WFPS treatments could be attributed to the degradation of the enzymes during storage (2 months). Thus, the rate of diffusion was likely constant between experiments 1 and 2 but the lower enzyme activity in experiment 2 allowed expression of a greater degree of fractionation.

**$N_2O$ reduction and source apportionment based on SP**

In this study, isotopic discrimination during reduction of $N_2O$ was observed in SP and the ε values ranged from -4.5 to 0 ‰ (Table 2 and 4). This is in contrast to studies of $N_2O$ production, which showed no discrimination in SP (Sutka et al, 2006; Toyoda et al., 2005). With the exception of experiment 2, the εSP value of -4.5 ‰ in experiment 1 is comparable to the values of -5.0 and -6.8 ‰ for pure cultures of *Pseudomonas stutzeri* and *Pseudomonas denitrificans* (Ostrom et al., 2007), and -6.4 ‰ from ocean environments (Yamagishi et al., in press). Fractionation in SP during $N_2O$ reduction is problematic in source apportionment studies that rely on constant SP values. For example, $N_2O$ reduction would cause an increase in SP from the value of 0 ‰ associated with production of $N_2O$ from denitrication towards that of 33 ‰ associated with production from nitrification (Sutka et al, 2006; Ostrom et al, 2007). Consequently, the effect on SP, $\delta^{15}N$ and $\delta^{18}O$ due to $N_2O$ reduction will ultimately affect source

apportionment and could become critical in regions or times with high rates of $N_2O$ reduction. The importance of this process remains unresolved as direct measures of $N_2O$ reduction in field studies are rare (Ostrom et al., 2007).

**The relationship between $\delta^{18}O$ and $\delta^{15}N$, and $\delta^{18}O$ and $\delta^{15}N^{\alpha}$**

Nitrous oxide reduction is a challenge to studies using stable isotopes to resolve the origins of this gas and, therefore, it is critical to establish a mean for recognizing when reduction is important. A potential means for recognizing $N_2O$ reduction resides in the relationship among $N_2O$ isotopologues. This study found a consistent relationship between $\delta^{18}O$ and $\delta^{15}N$ during reduction defined by a slope of 2.7 across all levels of WFPS (Figure 7). This relationship was present in experiments 1 and 2 despite differences in initial isotopologue values of the standards (tank A vs tank C) used to initiate $N_2O$ reduction. With respect to other $N_2O$ reduction studies in soils, the slope of 2.7 for $\delta^{18}O$ vs $\delta^{15}N$ agrees remarkably well with the slopes of 2.5 reported by Ostrom et al. (2007), 2.5 reported by Menyailo and Hungate (2006) and 2.0 reported by Mandernack et al. (2000).

This study, however, extends beyond previous work on $N_2O$ reduction by establishing a relationship between $\delta^{18}O$ and $\delta^{15}N^{\alpha}$ for the first time in soils. In response to the reduction of $N_2O$, $\delta^{18}O$ vs. $\delta^{15}N^{\alpha}$ is linearly correlated and displays a slope of 2.0 for all experiments. In $N_2O$ reduction in pure culture a slope of 1.7 for $\delta^{18}O$ vs. $\delta^{15}N^{\alpha}$ (Ostrom et al., 2007) was observed , which is comparable to the slope of 2.2 in this study. Thus, a definitive means of identifying when $N_2O$ reduction is predominant are

relationships between $\delta^{18}O$ and $\delta^{15}N$ and $\delta^{18}O$ and $\delta^{15}N^{\alpha}$ of 2.7 and 2.0, respectively. These relationships differ markedly from the slope of less than 1 common in flux chamber studies (for both $\delta^{18}O$ and $\delta^{15}N$ and $\delta^{18}O$ and $\delta^{15}N^{\alpha}$) (Ostrom et al., 2007).

## CONCLUSIONS

The isotopic composition of $N_2O$ has been used to define microbial sources of $N_2O$ and resolve global budgets of this important greenhouse gas (Kim and Craig, 1990; Perez et al., 2001; Sutka et al, 2006). $N_2O$ reduction is a challenge to the studies because the isotope signal of the various sources is altered during this reaction. Furthermore the variable nature of ε values indicates that the magnitude of isotope shifts during reduction is also variable, which undermines corrections for this reaction. For example, the ε values for all $N_2O$ isotopologues consistently decline with increasing WFPS during $N_2O$ reduction. Site preference has been proposed as a conservative tracer of the production of $N_2O$ from nitrification and denitrification (Sutka et al., 2006), however, this study demonstrated that $N_2O$ reduction alters SP ($\varepsilon \leq -4.5‰$) and potentially source signals. With the exception of SP, all mesocosm treatments demonstrated consistent declines in the ε values for $N_2O$ isotopolgues with increasing WFPS. A pragmatic method for recognizing that isotope signatures are altered during reduction is the relationships between $\delta^{18}O$ and $\delta^{15}N$, and $\delta^{18}O$ and $\delta^{15}N^{\alpha}$ that approach 2.7 and 2.2, respectively. These relationships do not vary with WFPS and may provide a means for correcting for reduction if and when it occurs.

# APPENDICES

**APPENDIX 1.** Ion current ratios of $N_2O$ measured over time for 60 (a), 80 (b) and 100 (c) % WFPS, experiment 1. All treatments were conducted in triplicates (R1, R2 and R3).

(A)

| WFPS (%) | Time elapsed (h) | Peak height of $N_2O$ | Peak height of NO | δ45/44 | δ46/44 | δ31/30 |
|---|---|---|---|---|---|---|
| 60R1 t0 | 0 | 12.62 | 3.45 | 0.46 | 0.14 | 2.43 |
| 60R1 t1 | 3 | 12.86 | 3.51 | 1.82 | 3.67 | 3.69 |
| 60R1 t2 | 7 | 8.56 | 2.33 | 6.37 | 14.2 | 8.99 |
| 60R2 t0 | 0 | 8.93 | 2.44 | 0.69 | 0.72 | 1.87 |
| 60R2 t1 | 4 | 7.57 | 2.07 | 3.33 | 6.17 | 5.27 |
| 60R2 t2 | 8 | 5.07 | 1.39 | 7.75 | 16.22 | 10.86 |
| 60R3 t0 | 0 | 10.84 | 2.96 | 0.41 | -0.04 | 1.62 |
| 60R3 t1 | 4 | 8.25 | 2.25 | 3.35 | 5.83 | 5.66 |
| 60R3 t2 | 9 | 5.19 | 1.43 | 7.58 | 16.72 | 9.96 |

**APPENDIX 1.** Continued

(B)

| WFPS (%) | Time elapsed (h) | Peak height of $N_2O$ | Peak height of NO | δ45/44 | δ46/44 | δ31/30 |
|---|---|---|---|---|---|---|
| 80R1 t0 | 0 | 10.9 | 2.98 | 0.44 | 0.12 | 1.87 |
| 80RI t1 | 3 | 11.52 | 3.14 | 1.36 | 1.51 | 2.82 |
| 80R1 t3 | 11 | 8.89 | 2.42 | 3.99 | 8.19 | 5.75 |
| 80R1 t4 | 14 | 11.94 | 3.26 | 5.81 | 12.9 | 7.5 |
| 80R1 t5 | 17 | 12.65 | 3.46 | 7.41 | 17.24 | 10.92 |
| 80R1 t6 | 19 | 8.98 | 2.46 | 10.76 | 23.72 | 12.48 |
| 80R1 t7 | 20 | 9.58 | 2.62 | 12.04 | 27.13 | 14.58 |
| 80R1 t8 | 21 | 14.23 | 3.91 | 12.68 | 30.04 | 16.8 |
| 80R2 t0 | 0 | 9.81 | 2.68 | 0.65 | -0.24 | 1.27 |
| 80R2 t1 | 4 | 8.24 | 2.25 | 1.99 | 3.2 | 4.54 |
| 80R2 t2 | 8 | 6.05 | 1.65 | 3.67 | 7.67 | 5.72 |
| 80R2 t3 | 12 | 6.28 | 1.72 | 7.04 | 13.63 | 9.09 |
| 80R2 t4 | 16 | 6.65 | 1.82 | 9.89 | 22.47 | 12.97 |
| 80R2 t5 | 18 | 5.88 | 1.61 | 13.35 | 30.41 | 15.34 |
| 80R3 t0 | 0 | 10.86 | 2.97 | 0.53 | -0.18 | 1.89 |
| 80R3 t1 | 4 | 10.17 | 2.78 | 1.61 | 2.05 | 3.74 |
| 80R3 t2 | 8 | 7.31 | 2 | 3.33 | 5.64 | 3.55 |
| 80R3 t3 | 12 | 7.12 | 1.95 | 5.49 | 10.63 | 6.3 |
| 80R3 t4 | 15 | 8.81 | 2.41 | 6.87 | 14.99 | 10.19 |
| 80R3 t5 | 17 | 9.46 | 2.59 | 8.78 | 19.48 | 11.04 |
| 80R3 t7 | 21 | 6.69 | 1.84 | 14.86 | 33.51 | 18.35 |
| 80R3 t8 | 22 | 8.22 | 2.26 | 16.74 | 36.93 | 21.39 |

**APPENDIX 1.** Continued

(C)

| WFPS (%) | Time elapsed (h) | Peak height of $N_2O$ | Peak height of NO | δ45/44 | δ46/44 | δ31/30 |
|---|---|---|---|---|---|---|
| 100R1 t0 | 0.000 | 11.36 | 3.1 | 0.44 | -0.06 | 1.74 |
| 100R1 t1 | 4.133 | 16.08 | 4.45 | 0.6 | 1.25 | 2.59 |
| 100R1 t2 | 8.317 | 13.5 | 3.69 | 1.34 | 2.47 | 3.39 |
| 100R1 t3 | 12.317 | 11.55 | 3.15 | 2 | 3.63 | 4.18 |
| 100R1 t4 | 16.133 | 18.82 | 5.33 | 2.36 | 6.12 | 4.56 |
| 100R1 t5 | 18.717 | 18.38 | 5.17 | 2.9 | 7.73 | 5.25 |
| 100R1 t6 | 21.200 | 14.3 | 3.93 | 3.81 | 9.26 | 5.29 |
| 100R1 t8 | 24.467 | 19.08 | 5.38 | 4.65 | 12.76 | 7.71 |
| 100R1 t9 | 26.367 | 16.05 | 4.42 | 5.8 | 15.48 | 8.82 |
| 100R1 t10 | 28.400 | 11.78 | 2.78 | 1.61 | 2.05 | 3.74 |
| 100R1 t11 | 29.650 | 13.97 | 3.84 | 8.85 | 22.04 | 3.84 |
| | | | | | | |
| 100R2 t0 | 0.000 | 10.48 | 2.86 | 0.59 | 0 | 1.48 |
| 100R2 t1 | 4.050 | 9.95 | 2.72 | 0.64 | 0.52 | 1.64 |
| 100R2 t2 | 8.183 | 9.32 | 2.55 | 1.24 | 1.29 | 2.52 |
| 100R2 t3 | 11.717 | 11.62 | 3.18 | 1.78 | 2.4 | 1.95 |
| 100R2 t4 | 15.367 | 17.9 | 5 | 1.65 | 3.72 | 3.82 |
| 100R2 t5 | 17.833 | 16.85 | 4.65 | 1.88 | 4.75 | 3.85 |
| 100R2 t6 | 20.350 | 14.23 | 3.9 | 2.5 | 5.46 | 4.35 |
| 100R2 t8 | 24.650 | 14.75 | 4.12 | 3.32 | 7.49 | 4.45 |
| 100R2 t10 | 28.167 | 16.87 | 4.79 | 4.6 | 11.27 | 7.14 |
| 100R2 t11 | 29.500 | 18.98 | 5.45 | 4.91 | 13.9 | 8.53 |
| | | | | | | |
| 100R3 t0 | 0.000 | 11.37 | 3.11 | 0.51 | -0.33 | 2.13 |
| 100R3 t1 | 4.100 | 9.26 | 2.53 | 1.04 | 0.48 | 1.34 |
| 100R3 t2 | 8.267 | 9.55 | 2.61 | 1.06 | 1.67 | 2.82 |
| 100R3 t3 | 11.983 | 11.13 | 3.04 | 1.84 | 2.92 | 3.54 |
| 100R3 t4 | 15.100 | 16.7 | 4.62 | 1.85 | 3.74 | 3.53 |
| 100R3 t5 | 17.567 | 17.07 | 4.73 | 1.91 | 4.42 | 3.9 |
| 100R3 t6 | 20.133 | 14.73 | 4.04 | 2.72 | 5.28 | 5.09 |
| 100R3 t8 | 23.950 | 11.51 | 3.17 | 3.65 | 6.84 | 5.23 |
| 100R3 t9 | 26.283 | 19.68 | 5.65 | 3.49 | 8.81 | 6.11 |
| 100R3 t10 | 27.933 | 18.38 | 5.26 | 3.95 | 9.61 | 6.82 |

**APPENDIX 2.** Isotopic compositions of $N_2O$ isotopologues for 60 (a), 80 (b) and 100 (c) % WFPS. The δ values were calculated from the ion current ratios with reference to VSMOW and air (Toyoda and Yoshida, 1999). All treatments were conducted in triplicate (R1, R2 and R3)

(A)

| WFPS (%) | Time elapsed (h) | $\delta^{15}N$ | $\delta^{15}N^{\alpha}$ | $\delta^{15}N^{\beta}$ | $\delta^{18}O$ |
|---|---|---|---|---|---|
| 60R1 t0 | 0 | 2.06 | 17.61 | -13.49 | 41.81 |
| 60R1 t1 | 3 | 3.4 | 18.84 | -12.03 | 45.49 |
| 60R1 t2 | 7 | 7.92 | 24.24 | -8.39 | 56.47 |
| 60R2 t0 | 0 | 2.29 | 16.94 | -12.36 | 42.41 |
| 60R2 t1 | 4 | 4.93 | 20.48 | -10.62 | 48.09 |
| 60R2 t2 | 8 | 9.33 | 26.24 | -7.59 | 58.57 |
| 60R3 t0 | 0 | 2.01 | 16.7 | -12.67 | 41.62 |
| 60R3 t1 | 4 | 4.96 | 20.94 | -11.02 | 47.74 |
| 60R3 t2 | 9 | 9.13 | 25.19 | -6.92 | 59.10 |

**APPENDIX 2.** Continued

(B)

| WFPS (%) | Time elapsed (h) | $\delta^{15}N$ | $\delta^{15}N^{\alpha}$ | $\delta^{15}N^{\beta}$ | $\delta^{18}O$ |
|---|---|---|---|---|---|
| 80R1 t0 | 0 | 2.04 | 16.97 | -12.89 | 41.79 |
| 80RI t1 | 3 | 2.97 | 17.97 | -12.02 | 43.23 |
| 80R1 t3 | 11 | 5.57 | 20.9 | -9.76 | 50.2 |
| 80R1 t4 | 14 | 7.37 | 22.62 | -7.88 | 55.12 |
| 80R1 t5 | 17 | 8.94 | 26.26 | -8.38 | 59.65 |
| 80R1 t6 | 19 | 12.3 | 27.63 | -3.02 | 66.39 |
| 80R1 t7 | 20 | 13.56 | 29.38 | -2.7 | 69.95 |
| 80R1 t8 | 21 | 14.16 | 32.2 | -3.87 | 73 |
| | | | | | |
| 80R2 t0 | 0 | 2.27 | 16.3 | -11.76 | 41.41 |
| 80R2 t1 | 4 | 3.59 | 19.83 | -12.64 | 45 |
| 80R2 t2 | 8 | 5.25 | 20.9 | -10.41 | 49.66 |
| 80R2 t3 | 12 | 8.64 | 24.37 | -7.08 | 55.86 |
| 80R2 t4 | 16 | 11.42 | 28.28 | -5.44 | 65.1 |
| 80R2 t5 | 18 | 14.86 | 30.49 | -0.77 | 73.37 |
| | | | | | |
| 80R3 t0 | 0 | 2.14 | 17.01 | -12.72 | 41.47 |
| 80R3 t1 | 4 | 3.22 | 18.98 | -12.54 | 43.8 |
| 80R3 t2 | 8 | 4.94 | 18.54 | -8.65 | 47.54 |
| 80R3 t3 | 12 | 7.09 | 21.37 | -7.19 | 52.74 |
| 80R3 t4 | 15 | 8.43 | 25.56 | -8.7 | 57.29 |
| 80R3 t5 | 17 | 10.33 | 26.25 | -5.6 | 61.98 |
| 80R3 t7 | 21 | 16.37 | 33.74 | -1 | 76.6 |
| 80R3 t8 | 22 | 18.27 | 37 | -0.47 | 80.16 |

**APPENDIX 2.** Continued

(C)

| WFPS (%) | Time elapsed (h) | $\delta^{15}N$ | $\delta^{15}N^{\alpha}$ | $\delta^{15}N^{\beta}$ | $\delta^{18}O$ |
|---|---|---|---|---|---|
| 100R1 t0 | 0 | 2.05 | 16.83 | -12.74 | 41.6 |
| 100R1 t1 | 4 | 2.18 | 17.73 | -13.38 | 42.97 |
| 100R1 t2 | 8 | 2.93 | 18.57 | -12.71 | 44.24 |
| 100R1 t3 | 12 | 3.59 | 19.4 | -12.21 | 45.45 |
| 100R1 t4 | 16 | 3.91 | 19.69 | -11.88 | 48.06 |
| 100R1 t5 | 19 | 4.43 | 20.38 | -11.51 | 49.74 |
| 100R1 t6 | 21 | 5.35 | 20.33 | -9.62 | 51.33 |
| 100R1 t8 | 24 | 6.15 | 22.89 | -10.60 | 54.99 |
| 100R1 t9 | 26 | 7.29 | 23.99 | -9.41 | 57.83 |
| 100R1 t10 | 28 | 9.19 | 26.17 | -7.79 | 61.41 |
| 100R1 t11 | 30 | 10.33 | 27.86 | -7.19 | 64.66 |
| | | | | | |
| 100R2 t0 | 0 | 2.2 | 16.53 | -12.13 | 41.66 |
| 100R2 t1 | 4 | 2.24 | 16.68 | -12.20 | 42.21 |
| 100R2 t2 | 8 | 2.85 | 17.64 | -11.93 | 43 |
| 100R2 t3 | 12 | 3.39 | 16.91 | -10.13 | 44.16 |
| 100R2 t4 | 15 | 3.22 | 18.99 | -12.54 | 45.55 |
| 100R2 t5 | 18 | 3.44 | 18.96 | -12.09 | 46.63 |
| 100R2 t6 | 20 | 4.07 | 19.48 | -11.34 | 47.36 |
| 100R2 t8 | 25 | 4.88 | 19.47 | -9.70 | 49.48 |
| 100R2 t10 | 28 | 6.13 | 22.32 | -10.05 | 53.43 |
| 100R2 t11 | 30 | 6.39 | 23.76 | -10.98 | 56.18 |
| | | | | | |
| 100R3 t0 | 0 | 2.13 | 17.29 | -13.04 | 41.32 |
| 100R3 t1 | 4 | 2.66 | 16.33 | -11.01 | 42.16 |
| 100R3 t2 | 8 | 2.65 | 17.96 | -12.66 | 43.41 |
| 100R3 t3 | 12 | 3.44 | 18.7 | -11.82 | 44.71 |
| 100R3 t4 | 15 | 3.43 | 18.65 | -11.79 | 45.57 |
| 100R3 t5 | 18 | 3.48 | 19.04 | -12.08 | 46.28 |
| 100R3 t6 | 20 | 4.31 | 20.33 | -11.72 | 47.17 |
| 100R3 t8 | 24 | 5.25 | 20.39 | -9.89 | 48.79 |
| 100R3 t9 | 26 | 5.03 | 21.3 | -11.24 | 50.86 |
| 100R3 t10 | 28 | 5.49 | 22.06 | -11.07 | 51.69 |

**APPENDIX 3.** Isotopic compositions (corrected δ values) of $N_2O$ isotopologues, isotopomers and site preference (SP) for 60 (a), 80 (b) and 100 (c) % WFPS, experiment 1). All treatments were conducted in triplicate (R1, R2 and R3)

(A)

| WFPS (%) | Time elapsed (h) | $\delta^{15}N$ | $\delta^{15}N^{\alpha}$ | $\delta^{15}N^{\beta}$ | SP |
|---|---|---|---|---|---|
| 60R1 t0 | 0 | 1.5 | 15.32 | -12.32 | 27.64 |
| 60R1 t1 | 3 | 2.84 | 16.55 | -10.87 | 27.42 |
| 60R1 t2 | 7 | 7.36 | 21.95 | -7.23 | 29.18 |
| 60R2 t0 | 0 | 1.73 | 14.65 | -11.19 | 25.84 |
| 60R2 t1 | 4 | 4.37 | 18.92 | -10.18 | 29.1 |
| 60R2 t2 | 8 | 8.66 | 24.15 | -6.83 | 30.98 |
| 60R3 t0 | 0 | 1.45 | 14.41 | -11.51 | 25.92 |
| 60R3 t1 | 4 | 4.4 | 19.38 | -10.58 | 29.96 |
| 60R3 t2 | 9 | 8.46 | 23.1 | -6.18 | 29.28 |

**APPENDIX 3.** Continued

(B)

| WFPS (%) | Time elapsed (h) | $\delta^{15}N$ | $\delta^{15}N^{\alpha}$ | $\delta^{15}N^{\beta}$ | SP |
|---|---|---|---|---|---|
| 80R1 t0 | 0 | 1.48 | 14.68 | -11.72 | 26.40 |
| 80RI t1 | 3 | 2.41 | 15.68 | -10.86 | 26.54 |
| 80R1 t3 | 11 | 5.01 | 18.61 | -8.59 | 27.2 |
| 80R1 t4 | 14 | 6.81 | 20.33 | -6.71 | 27.04 |
| 80R1 t5 | 17 | 8.38 | 23.97 | -7.21 | 31.18 |
| 80R1 t6 | 19 | 11.74 | 25.34 | -1.86 | 27.20 |
| 80R1 t7 | 20 | 13.00 | 27.09 | -1.09 | 28.18 |
| 80R1 t8 | 21 | 13.6 | 29.91 | -2.71 | 32.62 |
| 80R2 t0 | 0 | 1.71 | 14.01 | -10.59 | 24.6 |
| 80R2 t1 | 4 | 3.03 | 17.54 | -11.48 | 29.02 |
| 80R2 t2 | 8 | 4.69 | 19.34 | -9.96 | 29.3 |
| 80R2 t3 | 12 | 7.97 | 22.28 | -6.34 | 28.62 |
| 80R2 t4 | 16 | 10.425 | 27.24 | -6.39 | 33.63 |
| 80R2 t5 | 18 | 13.865 | 29.45 | -1.72 | 31.17 |
| 80R3 t0 | 0 | 1.58 | 14.72 | -11.56 | 26.28 |
| 80R3 t1 | 4 | 2.66 | 16.69 | -11.37 | 28.06 |
| 80R3 t2 | 8 | 4.38 | 16.98 | -8.22 | 25.20 |
| 80R3 t3 | 12 | 6.42 | 19.28 | -6.44 | 25.72 |
| 80R3 t4 | 15 | 7.435 | 24.52 | -9.65 | 34.17 |
| 80R3 t5 | 17 | 9.335 | 25.21 | -6.54 | 31.75 |
| 80R3 t7 | 21 | 15.68 | 32.65 | -1.29 | 33.94 |
| 80R3 t8 | 22 | 17.58 | 35.91 | -0.75 | 36.66 |

**APPENDIX 3.** Continued

(C)

| WFPS (%) | Time elapsed (h) | $\delta^{15}N$ | $\delta^{15}N^{\alpha}$ | $\delta^{15}N^{\beta}$ | SP |
|---|---|---|---|---|---|
| 100R1 t0 | 0 | 1.49 | 14.54 | -11.56 | 26.10 |
| 100R1 t1 | 4 | 1.62 | 15.44 | -12.20 | 27.64 |
| 100R1 t2 | 8 | 2.37 | 16.28 | -11.54 | 27.82 |
| 100R1 t3 | 12 | 3.03 | 17.11 | -11.05 | 28.16 |
| 100R1 t4 | 16 | 3.35 | 17.40 | -10.70 | 28.10 |
| 100R1 t5 | 19 | 3.87 | 18.09 | -10.35 | 28.44 |
| 100R1 t6 | 21 | 4.79 | 18.04 | -8.46 | 26.50 |
| 100R1 t8 | 24 | 5.59 | 20.60 | -9.42 | 30.02 |
| 100R1 t9 | 26 | 6.73 | 21.70 | -8.24 | 29.94 |
| 100R1 t10 | 28 | 8.63 | 23.88 | -6.62 | 30.50 |
| 100R1 t11 | 30 | 9.77 | 25.57 | -6.03 | 31.60 |
| 100R2 t0 | 0 | 1.64 | 14.24 | -10.96 | 25.20 |
| 100R2 t1 | 4 | 1.68 | 15.12 | -11.76 | 26.88 |
| 100R2 t2 | 8 | 2.29 | 16.08 | -11.50 | 27.58 |
| 100R2 t3 | 12 | 2.72 | 14.82 | -9.38 | 24.20 |
| 100R2 t4 | 15 | 2.23 | 17.95 | -13.50 | 31.45 |
| 100R2 t5 | 18 | 2.45 | 17.92 | -13.03 | 30.95 |
| 100R2 t6 | 20 | 3.40 | 17.39 | -10.59 | 27.98 |
| 100R2 t8 | 25 | 4.19 | 18.38 | -10.00 | 28.38 |
| 100R2 t10 | 28 | 5.44 | 21.23 | -10.35 | 31.58 |
| 100R2 t11 | 30 | 5.70 | 22.67 | -11.27 | 33.94 |
| 100R3 t0 | 0 | 1.57 | 15.00 | -11.86 | 26.86 |
| 100R3 t1 | 4 | 2.10 | 14.77 | -10.57 | 25.34 |
| 100R3 t2 | 8 | 2.09 | 16.40 | -12.22 | 28.62 |
| 100R3 t3 | 12 | 2.77 | 16.61 | -11.07 | 27.68 |
| 100R3 t4 | 15 | 2.76 | 16.56 | -11.04 | 27.60 |
| 100R3 t5 | 18 | 2.49 | 18.00 | -13.03 | 31.03 |
| 100R3 t6 | 20 | 3.64 | 18.24 | -10.96 | 29.20 |
| 100R3 t8 | 24 | 4.56 | 19.30 | -10.18 | 29.48 |
| 100R3 t9 | 26 | 4.34 | 20.21 | -11.53 | 31.74 |
| 100R3 t10 | 28 | 4.80 | 20.97 | -11.37 | 32.34 |

**APPENDIX 4.** Headspace concentration data for 60, 80 and 100 % WFPS, experiment 1 over time. All treatments were conducted in triplicate (R1, R2 and R3).

| WFPS (%) | Total Elapsed (h) | Concentration (μmol) [Initial] | [Final] |
|---|---|---|---|
| 60R1 | 7 | 49.02 | 23.11 |
| 60R2 | 8 | 33.86 | 14.95 |
| 60R3 | 9 | 41.71 | 15.35 |
| Avg | | 41.53 | 17.80 |
| STD | | 7.59 | 4.60 |
| | | | |
| 80R1 | 17 | 41.95 | 13.69 |
| 80R2 | 18 | 37.47 | 4.92 |
| 80R3 | 17 | 41.79 | 8.23 |
| Avg | | 40.41 | 8.95 |
| STD | | 2.54 | 4.43 |
| | | | |
| 100R1 | 28 | 43.84 | 12.69 |
| 100R2 | 28 | 40.23 | 14.92 |
| 100R3 | 28 | 43.89 | 16.25 |
| Avg | | 42.65 | 14.62 |
| STD | | 2.10 | 1.80 |

**APPENDIX 5.** Ion current ratios of $N_2O$ measured over time for 60 (A) and 110 (B) % WFPS, experiment 2.

(A)

| WFPS (%) | Time elapsed (h) | Peak height of $N_2O$ | Peak height of NO | δ45/44 | δ46/44 | δ31/30 |
|---|---|---|---|---|---|---|
| 60 t0 | 0 | 11.57 | 3.30 | 1.42 | 0.09 | -3.68 |
| 60 t2 | 4 | 14.05 | 4.15 | 1.81 | 1.29 | 0.97 |
| 60 t3 | 5 | 11.00 | 3.14 | 1.75 | 1.52 | -1.24 |
| 60 t4 | 6 | 12.31 | 3.57 | 2.01 | 1.48 | -2.08 |
| 60 t5 | 8 | 13.42 | 3.95 | 2.54 | 2.97 | -0.17 |
| 60 t6 | 10 | 13.28 | 3.90 | 2.85 | 3.31 | 0.05 |
| 60 t7 | 11 | 11.69 | 3.38 | 2.34 | 3.81 | -2.31 |
| 60 t8 | 13 | 12.63 | 3.70 | 3.16 | 4.72 | -1.14 |
| 60 t9 | 15 | 12.29 | 3.60 | 3.24 | 5.33 | -0.89 |
| 60t10 | 18 | 12.83 | 3.76 | 4.52 | 6.11 | -0.92 |
| 60 t11 | 22 | 12.70 | 3.72 | 4.77 | 8.43 | -0.55 |
| 60 t12 | 25 | 12.17 | 3.53 | 5.53 | 9.59 | -0.60 |
| 60 t13 | 29 | 11.65 | 3.36 | 5.87 | 11.30 | -1.23 |
| 60 t14 | 33 | 11.75 | 3.39 | 7.23 | 13.68 | 1.14 |
| 60 t15 | 35 | 12.12 | 3.55 | 6.91 | 14.61 | 1.17 |
| 60 t16 | 38 | 14.80 | 4.43 | 8.43 | 16.48 | 5.66 |
| 60 t17 | 40 | 14.08 | 4.20 | 9.50 | 18.14 | 5.28 |
| 60 t19 | 49 | 14.45 | 4.35 | 12.29 | 25.98 | 11.55 |
| 60 t20 | 52 | 12.58 | 3.74 | 13.57 | 29.35 | 9.02 |
| 60 t21 | 55 | 11.93 | 3.53 | 14.90 | 33.93 | 13.50 |
| 60 t22 | 57 | 11.70 | 3.46 | 16.23 | 36.74 | 12.14 |
| 60 t23 | 59 | 11.84 | 3.53 | 16.60 | 40.37 | 15.47 |

**APPENDIX 5.** Continued.

(B)

| WFPS (%) | Time elapsed (h) | Peak height of $N_2O$ | Peak height of NO | δ45/44 | δ46/44 | δ31/30 |
|---|---|---|---|---|---|---|
| 110 t0 | 0 | 11.62 | 3.32 | 1.14 | 0.26 | -3.43 |
| 110 t2 | 12 | 14.00 | 4.13 | 1.93 | 1.31 | -1.47 |
| 110 t3 | 16 | 10.72 | 3.05 | 1.72 | 1.28 | -2.16 |
| 110 t4 | 21 | 13.48 | 3.95 | 2.62 | 2.50 | -1.04 |
| 110 t5 | 24 | 12.93 | 3.80 | 2.19 | 2.74 | -0.44 |
| 110 t6 | 28 | 12.23 | 3.58 | 2.47 | 3.47 | -3.24 |
| 110 t7 | 35 | 12.29 | 3.59 | 3.15 | 5.50 | -2.31 |
| 110 t8 | 42 | 11.22 | 3.21 | 4.51 | 8.76 | -2.13 |
| 110 t11 | 48 | 12.70 | 3.75 | 7.04 | 16.04 | 3.47 |
| 110 t12 | 49 | 12.23 | 3.58 | 8.32 | 18.40 | 4.38 |
| 110 t13 | 51 | 10.85 | 3.11 | 10.44 | 25.18 | 5.92 |
| 110 t14 | 52 | 9.57 | 2.73 | 11.96 | 29.50 | 6.21 |
| 110 t15 | 53 | 8.51 | 2.42 | 15.25 | 37.00 | 11.51 |

**APPENDIX 6.** Isotopic compositions of $N_2O$ isotopologues for 60 (A) and 110 (B) % WFPS. The δ values were calculated from the ion current ratios with reference to VSMOW and air (Toyoda and Yoshida, 1999).

(A)

| WFPS (%) | Time elapsed (h) | $\delta^{15}N$ | $\delta^{15}N^{\alpha}$ | $\delta^{15}N^{\beta}$ | $\delta^{18}O$ |
|---|---|---|---|---|---|
| 60 t0 | 0 | -1.47 | -3.46 | 4.57 | 37.92 |
| 60 t2 | 4 | -1.12 | 1.72 | 0.14 | 38.88 |
| 60 t3 | 5 | -1.56 | -0.78 | 2.51 | 39.48 |
| 60 t4 | 6 | -1.37 | -1.74 | 4.02 | 39.29 |
| 60 t5 | 8 | -1.21 | 0.33 | 2.99 | 40.71 |
| 60 t6 | 10 | -1.23 | 0.55 | 3.40 | 41.07 |
| 60 t7 | 11 | -1.46 | -2.13 | 4.98 | 41.79 |
| 60 t8 | 13 | -1.32 | -0.87 | 5.40 | 42.62 |
| 60 t9 | 15 | -1.37 | -0.63 | 5.29 | 43.29 |
| 60t10 | 18 | -1.29 | -0.73 | 8.05 | 44.03 |
| 60 t11 | 22 | -1.31 | -0.44 | 8.16 | 46.46 |
| 60 t12 | 25 | -1.39 | -0.58 | 9.84 | 47.72 |
| 60 t14 | 33 | -1.45 | 1.13 | 11.49 | 52.02 |
| 60 t15 | 35 | -1.40 | 1.13 | 10.77 | 52.96 |
| 60 t16 | 38 | -1.01 | 6.07 | 8.93 | 54.58 |
| 60 t17 | 40 | -1.12 | 5.56 | 11.64 | 56.38 |
| 60 t19 | 49 | -1.06 | 12.14 | 10.49 | 64.50 |
| 60 t20 | 52 | -1.33 | 9.07 | 16.07 | 68.21 |
| 60 t21 | 55 | -1.42 | 13.87 | 13.84 | 73.06 |
| 60 t22 | 57 | -1.46 | 12.15 | 18.20 | 76.01 |
| 60 t23 | 59 | -1.44 | 15.72 | 15.23 | 79.78 |

**APPENDIX 6.** Continued.

(B)

| WFPS (%) | Time elapsed (h) | $\delta^{15}N$ | $\delta^{15}N^{\alpha}$ | $\delta^{15}N^{\beta}$ | $\delta^{18}O$ |
|---|---|---|---|---|---|
| 110 t0 | 0 | -1.47 | -3.18 | 3.69 | 38.10 |
| 110 t2 | 12 | -1.13 | -1.04 | 3.16 | 38.91 |
| 110 t3 | 16 | -1.60 | -1.81 | 3.49 | 39.26 |
| 110 t4 | 21 | -1.20 | -0.63 | 4.14 | 40.20 |
| 110 t5 | 24 | -1.28 | 0.04 | 2.55 | 40.52 |
| 110 t6 | 28 | -1.38 | -3.17 | 6.31 | 41.36 |
| 110 t7 | 35 | -1.37 | -2.24 | 6.70 | 43.47 |
| 110 t8 | 42 | -1.52 | -2.24 | 9.40 | 46.98 |
| 110 t11 | 48 | -1.31 | 3.65 | 8.45 | 54.39 |
| 110 t12 | 49 | -1.38 | 4.52 | 10.14 | 56.88 |
| 110 t13 | 51 | -1.58 | 5.86 | 12.92 | 64.10 |
| 110 t14 | 52 | -1.76 | 5.93 | 15.82 | 68.75 |
| 110 t15 | 53 | -1.91 | 11.45 | 16.83 | 76.66 |

**APPENDIX 7.** Isotopic compositions (corrected δ values) of $N_2O$ isotopologues, isotopomers and site preference (SP) for 60 (A) and 110 (B) % WFPS, experiment 2.

(A)

| WFPS (%) | Time elapsed (h) | $\delta^{15}N$ | $\delta^{15}N^{\alpha}$ | $\delta^{15}N^{\beta}$ | SP |
|---|---|---|---|---|---|
| 60 t0 | 0 | -0.91 | 1.38 | -3.21 | 4.59 |
| 60 t2 | 4 | -0.18 | 6.56 | -6.92 | 13.48 |
| 60 t3 | 5 | -0.69 | 4.06 | -5.43 | 9.50 |
| 60 t4 | 6 | -0.23 | 3.10 | -3.56 | 6.66 |
| 60 t5 | 8 | 0.45 | 5.17 | -4.27 | 9.44 |
| 60 t6 | 10 | 0.75 | 5.39 | -3.89 | 9.28 |
| 60 t7 | 11 | -0.03 | 2.71 | -2.77 | 5.48 |
| 60 t8 | 13 | 0.95 | 3.97 | -2.08 | 6.05 |
| 60 t9 | 15 | 0.97 | 4.21 | -2.27 | 6.49 |
| 60t10 | 18 | 2.37 | 4.11 | 0.62 | 3.49 |
| 60 t11 | 22 | 2.55 | 4.40 | 0.69 | 3.71 |
| 60 t12 | 25 | 3.24 | 4.26 | 2.22 | 2.04 |
| 60 t14 | 33 | 4.86 | 5.97 | 3.75 | 2.22 |
| 60 t15 | 35 | 4.55 | 5.97 | 3.14 | 2.84 |
| 60 t16 | 38 | 6.49 | 10.91 | 2.06 | 8.85 |
| 60 t17 | 40 | 7.47 | 10.37 | 4.58 | 5.80 |
| 60 t19 | 49 | 10.26 | 16.98 | 3.53 | 13.45 |
| 60 t20 | 52 | 11.25 | 13.91 | 8.59 | 5.32 |
| 60 t21 | 55 | 12.44 | 18.71 | 6.16 | 12.55 |
| 60 t22 | 57 | 13.72 | 16.99 | 10.46 | 6.54 |
| 60 t23 | 59 | 14.04 | 20.56 | 7.53 | 13.04 |

**APPENDIX 7.** Continued.

(B)

| WFPS (%) | Time elapsed (h) | $\delta^{15}N$ | $\delta^{15}N^{\alpha}$ | $\delta^{15}N^{\beta}$ | SP |
|---|---|---|---|---|---|
| 110 t0 | 0 | -1.21 | 1.66 | -4.08 | 5.74 |
| 110 t2 | 12 | -0.07 | 3.80 | -3.94 | 7.74 |
| 110 t3 | 16 | -0.76 | 3.03 | -4.54 | 7.58 |
| 110 t4 | 21 | 0.56 | 4.21 | -3.09 | 7.31 |
| 110 t5 | 24 | 0.02 | 4.88 | -4.84 | 9.72 |
| 110 t6 | 28 | 0.20 | 1.67 | -1.27 | 2.94 |
| 110 t7 | 35 | 0.87 | 2.60 | -0.86 | 3.47 |
| 110 t8 | 42 | 2.06 | 2.60 | 1.51 | 1.09 |
| 110 t11 | 48 | 4.74 | 8.49 | 0.98 | 7.51 |
| 110 t12 | 49 | 5.96 | 9.36 | 2.56 | 6.80 |
| 110 t13 | 51 | 7.81 | 10.70 | 4.92 | 5.78 |
| 110 t14 | 52 | 9.12 | 10.77 | 7.47 | 3.30 |
| 110 t15 | 53 | 12.24 | 16.29 | 8.19 | 8.11 |

**APPENDIX 8.** Headspace concentration data for 60 and 110 % WFPS, experiment 2 over time.

| WFPS | Total Elapsed | Concentrations (mM) | |
|---|---|---|---|
| (%) | (h) | [initial] | [final] |
| 60 | 59 | 46.80 | 6.70 |
| 110 | 53 | 47.10 | 4.30 |

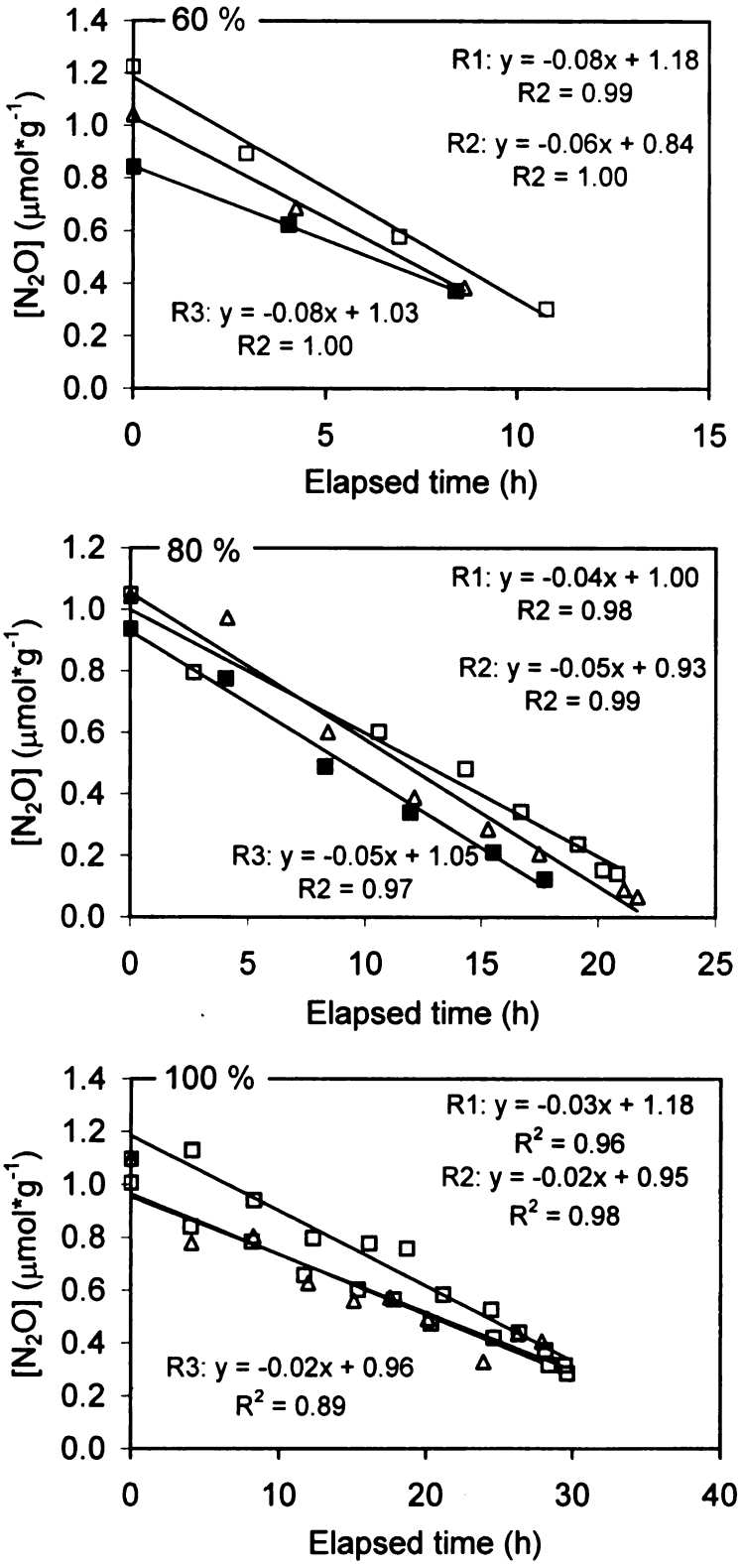


**APPENDIX 9.** Rate of N2O reduction for 60, 80 and 100 % WFPS, experiment 1 for replicate 1 (open square), replicate 2 (closed square) and replicate 3 (open triangle)

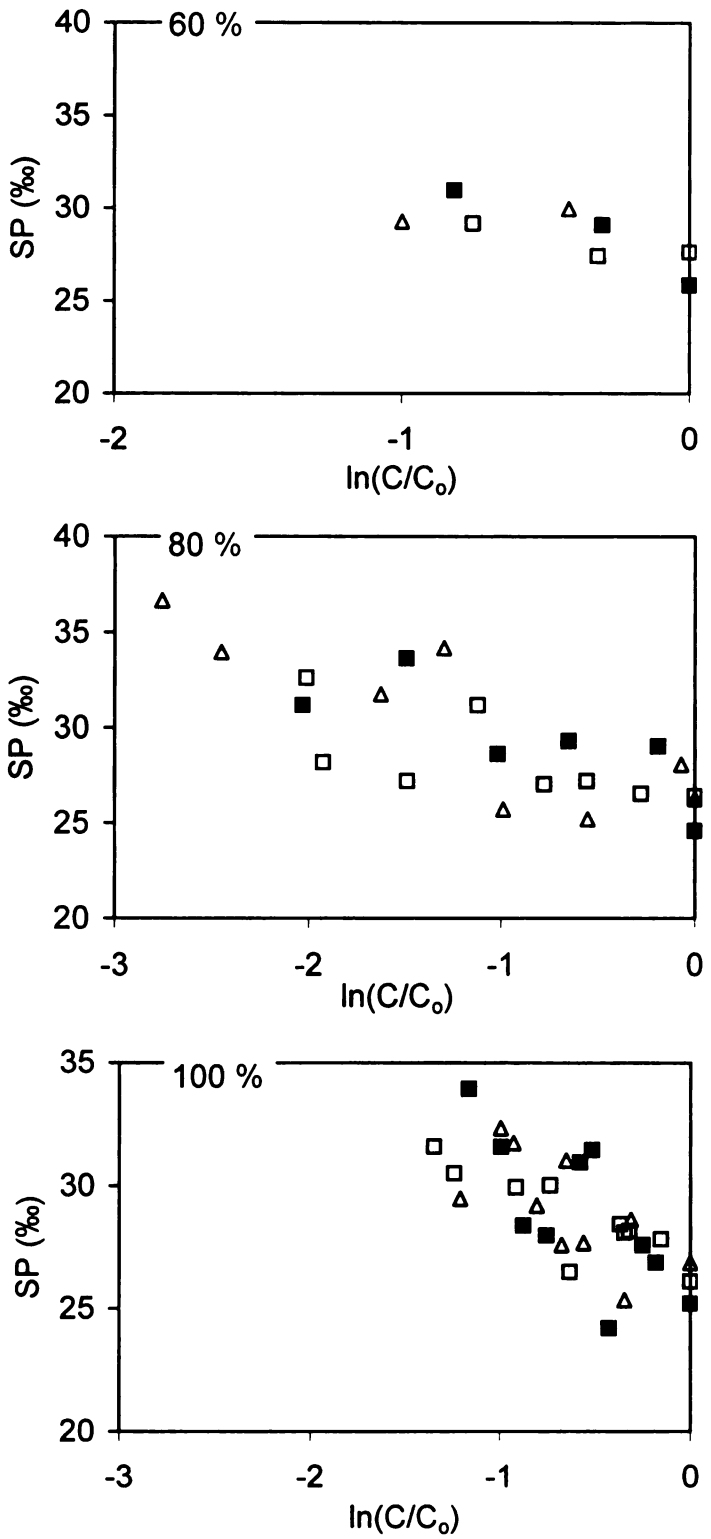


**APPENDIX 10.** Site preference as a function of $\ln(C/C_0)$ for 60, 80 and 100 % WFPS, experiment 1 for replicate 1 (open square), replicate 2 (closed square) and replicate 3 (open triangle).

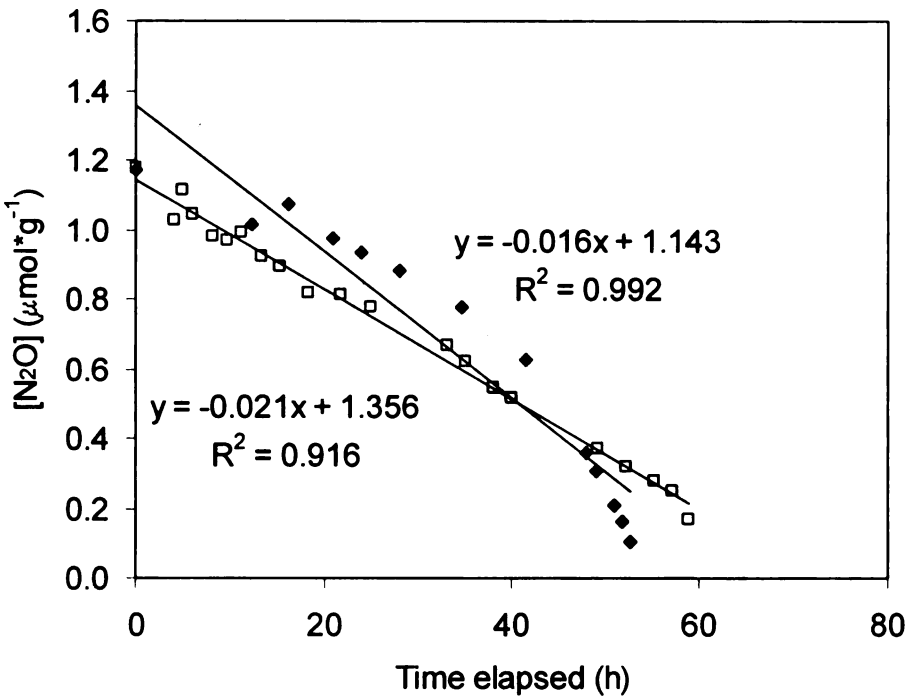


**APPENDIX 11.** Rate of $N_2O$ reduction for 60 (open square) and 110 (closed triangle) % WFPS over time, experiment 2.

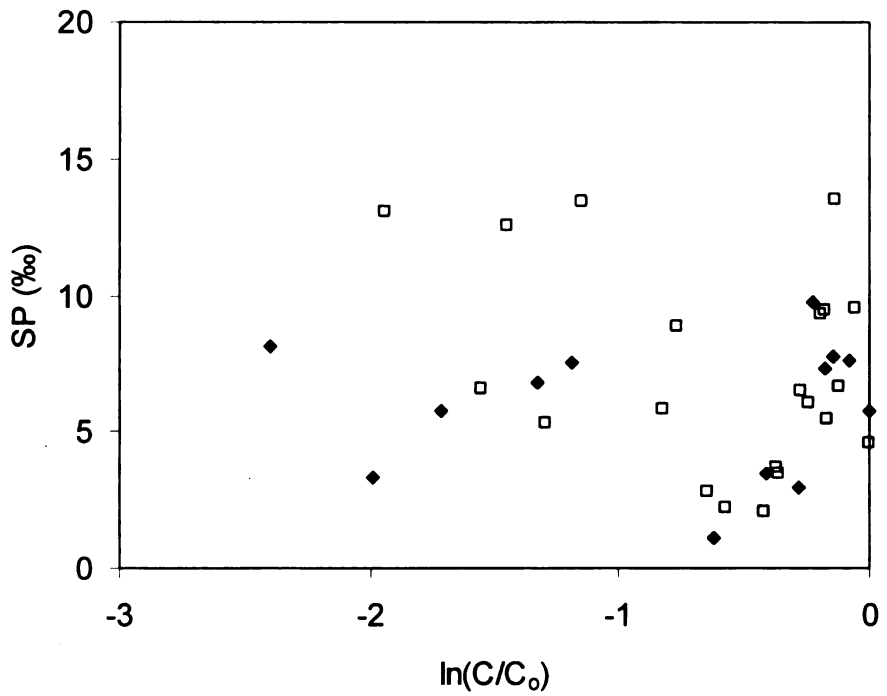


**APPENDIX 12.** Site preference (SP) as a function of $\ln(C/C_0)$ for 60 (open square) and 110 (closed triangle) % WFPS over time, experiment 2.

# REFERENCES

## REFERENCES


Barford, C.C., Montoya, J.P., Altabet, M.A. and Mitchell, R., 1999, Steady-state nitrogen isotope effect of $N_2$ and $N_2O$ production in *Paracoccus denitrificans*. Applied Environmental Microbiology, v. 65, p. 989-994.

Bergsma, T.T., Robertson, G.P. and Ostrom, N.E., 2002, Influence of soil moisture and land use history on denitrification end products. Journal of Environmental Quality, v. 31, p. 711-717.

Brandes, J.A., and Devol A.H., 1997, Isotopic fractionation of oxygen and nitrogen in coastal marine sediments. Geochimica et Cosmochimica Acta, v. 61, p. 1793-1801.

Cavagelli, M.A. and Robertson, G.P., 2000, Role of denitrifier diversity in rates of nitrous oxide consumption in a terrestrial ecosystem. Soil Biology & Biochemistry, v. 33, p. 297-310.

Dala, R., Wang, W., Robertson, G.P., Parton, W.J., Myer, M.C. and Raison, J.R., 2003, Emission sources of nitrous oxide from Australian agricultural and forest lands and mitigation options. National Carbon Accounting System. Technical report No. 35. Australian Greenhouse Office.

Elliott, E.T., Heil, J.W., Kelly, E.F. and Monger, H.C., 1999, Soil Structural and other physical properties, in Standard soil methods for long-term ecological research, Robertson , G.P., Coleman D.C., Bledsoe C.S. and Sollins P., eds., Oxford University Press, New York, p. 74-85.

Firestone, M.K. and Davidson, E.A., 1989, Microbiological basis of NO and $N_2O$ production and consumption in soil, *In*: Exchange of Trace Gases Between Ecosystems and the Atmosphere, Andreae, M.O., and Schimel, D.S., eds., John Wiley & Sons, New York, p. 7-21.

Groffman, P. M., Altabet, M.A., Bohlke, J. K., Bahl, K.B., David M.B., Firestone, M.K., Giblin, A.E., Kana, T. M., Nielsen, L. P. and Voytek, M. A., 2006, Methods for measuring denitrification: diverse approaches to a difficult problem. Ecological Application, v. 16, no. 6, p. 2091-2122.

Intergovernmental Panel on Climate Change (IPCC), 2001, Climate Change 2001: The scientific basis: Contribution of Working Group I to the third assessment report of the Intergovernmental Panel on Climate Change. J.T. Haughton Ed.; Cambridge University Press, New York, New York.

Kim, K.R., and Craig, H., 1990, Two isotope characterization of $N_2O$ in Pacific Ocean and constraints on its origin in deep water. Nature, v. 347, p. 58-60.

Mandernack, K.W. and Rahn, T., 2000, The biogeochemical controls of the $\delta^{15}N$ and $\delta^{18}O$ of $N_2O$ produced in landfill cover soils. Journal of Geophysical Research, v. 105, no. D14, p. 17709-17720.

Mariotti A., Germon, J.C, Hubert, P., Kaiser, P., Letolle, R., Tardieux, A. and Tardieux, P., 1981, Experimental determination of nitrogen kinetic isotope fractionations: Some principles; illustration for the denitrification and nitrification processes. Plant Soil, v. 62, p. 413-430.

Menyailo, O.V. and Hungate, B.A., 2006, Stable isotope discrimination during soil denitrification: production and consumption of nitrous oxide. Global Biogeochemical Cycles, v. 20, doi:10.1029/2005GB002527.

Minschwaner, K.R., Carver, R.W., Briegleb, B.P. and Roche, A.E., 1998, Infrared radiative forcing and atmospheric lifetimes of trace species based on observations from UARS. Journal of Geophysical Research, v. 103, p. 23243-23253.

Mosier, A.R., and Kroeze, C., 1998, A new approach to estimate emissions of nitrous oxide from agriculture and its implications to the global $N_2O$ budget. Global Change Newsletter, v. 34, p. 8-14.

Nevison, C., and Holland, E., 1997, Reexamination of the impact of anthropogenically fixed nitrogen on atmospheric $N_2O$ and the stratospheric $O_3$ layer. Geophysical Research Letter, v. 102, p. 25519-25536.

Olsen, S., McLinden, C. and Prather, M., 2001, Stratospheric $N_2O$-NOy system: testing uncertainties in a three-dimensional framework. Journal of Geophysical Research-Atmosphere, v. 106 no. D22, p. 28771-28784.

Ostrom, N.E., Hedin, L.O., VonFischer, J.C. and Robertson G.P.,2002, Nitrogen transformation and $NO_3^-$ removal at a soil-stream interface: A stable isotope approach. Ecological Applications, v. 12, p. 1027-1043.

Ostrom, N.E., Pitt, A., Sutka, R., Ostrom, P.H., Grandy, A.S., Huizinga, K.M., and Robertson, G.P., 2007, Isotopologue effects during $N_2O$ reduction in soils and in pure cultures of denitrifiers. Journal of Geophysical Research, v.112, doi:10.1029/2006JGR000287.

Prather, M., Gauss M., Berntsen, T., Isaksen, I., Sundet, J., Bey, I., Brasseur, G., Dentener, F., Derwent, R., Stevenson, D., Grenfell, L., Hauglustaine, D., Horowitz, L., Jacob, D., Mickley, L., Lawrence, M., von Kuhlmann, R., Muller, J. F., Pitari, G., Rogers, H., Johnson, M., Pyle, J., Law, K., van Weele, M., and Wild, O., 2003, Fresh air in the 21$^{st}$ century. Geophysical Research Letter, v. 30, no. 2, doi:10.1029/2002GL016285.

Perez, T., Trumbore, S.E., Tyler, S.C., Davidson, E.A., Keller, M. and de Camargo, P.B., 2000, Isotopic variability of $N_2O$ emissions from tropical forest soils. Global Biogeochemical Cycles, v. 14, p. 525-535.

Perez, T., Trumbore, S.E., Tyler, S.C., Matson, P.A., Ortiz-Monasterio, I., Rahn, T., and Griffith, D.W.T., 2001, Identifying the agricultural imprint on the global $N_2O$ budget using stable isotopes. Journal of Geophysical Research, v. 106, p. 9869-9878.

Prinn R., Cunnold D., Rasmussen, R., Simmonds, P., Alear, F., Fraser, P. and Rosen, R., 1990, Atmospheric trends and emissions of nitrous oxide deduced from ten years of ALE-GAGE data. Journal of Geophysical Research, v. 99, p. 5285.

Rasmussen, R.A. and Khalil, M.A.K., 1986, Atmospheric Trace Gases: Trends and Distributions Over the Last Decade. Science, v. 232, p. 1623.

Schmidt, H.L., Werner, R.A., Yoshida, N., Well, R., 2004, Is the isotopic composition of nitrous oxide an indicator for its origin from nitrification or denitrification? A theoretical approach from referred data and microbiological and enzyme kinetic aspects. Rapid Communication Mass Spectrometry, v. 18, p. 2036-2040.

Stein, L.Y. and Yung, Y.L., 2003, Production, isotopic composition, and atmospheric fate of biologically produced nitrous oxide. Global Biogeochemistry Cycle, v. 14, p. 537-543.

Sutka, R.L., Ostrom, N.E., Ostrom, P.H., Breznak, J.A., Gandhi, H., 2003, Nitrogen isotopomer site preference of $N_2O$ produced by *Nitrosomonas europaea* and *Methylococcus capsulats* Bath. Rapid Communication Mass Spectrometry, v. 17, p. 738-745.

Sutka, R.L., Ostrom, N.E., Ostrom, P.H., Breznak, J.A., Gandhi, H., Pitt, A.J., and Li, F., 2006, Distinguishing nitrous oxide production from nitrification and denitrification on the basis of isotopomer abundance. Applied and Experimental Microbiology, v. 72, p. 638-644.

Tilsner, J., Wrage, N., Lauf, J. and Gebauer, G., 2003, Emission of gaseous nitrogen oxides from an extensively managed grassland in NE Bavaria, Germany II. Stable isotope natural abundance of $N_2O$. Biogeochemistry, v. 67, p. 249-267.

Toyoda,S. and Yoshida N., 1999, Determination of nitrogen isotopomers of nitrous oxide on a modified isotope ratio mass spectrometer. Analytical Chemistry, v. 71, p. 4711-4718.

Toyoda S., Mutobe H., Yamagishi H., Yoshida N. and Tanji Y., 2005, Fractionation of $N_2O$ isotopomers during production by denitrifier. Soil Biology Biochemistry, v.37, p. 1535-1545.

Wahlen, M. and Yoshinari, T., 1985, Oxygen isotope ratios in $N_2O$ from different environments. Nature, v. 313, p. 780-782.

Wrage, N., Lauf, J., del Prado, A., Pinto, M., Pietrzak, S., Yamulki, S., Oenema, O, and Gebauer, G., 2004a, Distinguishing sources of $N_2O$ in European grasslands by stable isotope analysis. Rapid Communication Mass Spectrometry, v. 18, p. 1201-1207.
Wrage, N., Velthof, G.L., van Beusichem, M.L. and Oenema, O., 2001, Role of nitrifier denitrification in the production of nitrous oxide. Soil Biology and Biochemistry, v. 33, p. 1723-1732

Wrage N., Velthof, G.L., Laanbroekc, H.J. and Oenema, O., 2004b, Nitrous oxide production in grassland soils: assessing the contribution of nitrifier denitrification. Soil Biology and Biochemistry, v. 36, p. 229-236.

Wrage N., Velthof, G.L., Oenema, O., and Laanbroekc, H.J., 2004c, Acetylene and oxygen as inhibitors of nitrous oxide production in *Nitrosomonas europaea* and *Nitrosospira briensis*: a cautionary tale. FEMS Microbiology Ecology, v. 47, p. 13-18.

Yamagishi, H., Westley, M.B., Popp, B.N., Toyoda, S., Yoshida, N., Watanabe, S., Koba, K. and Yamanaka, Y., in press, Role of nitrification and denitrification on the nitrous oxide cycle in the eastern tropical North Pacific and Gulf of California,

Yamazaki, T., Yoshida, N., Wada, E. and Matsuo, S., 1987, $N_2O$ reduction by *Azobacter vinelandii* with emphasis on kinetic nitrogen isotope effects. Plant Cell Physiology, v. 28, p. 263-271.

Yoshida, N., Hattori, A., Saino, T., Matsuo, S. and Wada, E., 1984, $^{15}N/^{14}N$ ratio of dissolved $N_2O$ in the eastern tropical Pacific Ocean. Nature, v 307, p. 442-444.

Yoshida, N. and Toyoda, S., 2000, Contraining the atmospheric $N_2O$ budget from intramolecular site preference in $N_2O$. Nature. v. 405, p. 330-334.

Yung, Y.L. and Miller, C.E., 1997, Isotopic fractionation of stratospheric nitrous oxide. *Science*. v. 278, p. 1778-1780.